
Neural Force Field: Few-shot Learning of Generalized Physical Reasoning

Shiqian Li^{*,1}

shiqianli@stu.pku.edu.cn

Ruihong Shen^{*,1}

shen.ruihong@stu.pku.edu.cn

Yaoyu Tao^{1,✉}

taoyao@pku.edu.cn

Chi Zhang^{1,✉}

wellyzhang@gmail.com

Yixin Zhu^{1,✉}

yixin.zhu@pku.edu.cn

* equal contributors ✉ corresponding authors ¹ Institute for Artificial Intelligence, Peking UniversityProject website <https://neuralforcefield.github.io/>

Abstract

Physical reasoning is a remarkable human ability that enables rapid learning and generalization from limited experience. Current AI models, despite extensive training, still struggle to achieve similar generalization, especially in Out-of-distribution (OOD) settings. This limitation stems from their inability to abstract core physical principles from observations. A key challenge is developing representations that can efficiently learn and generalize physical dynamics from minimal data. Here we present Neural Force Field (NFF), a framework extending Neural Ordinary Differential Equation (NODE) to learn complex object interactions through **force field** representations, which can be efficiently integrated through an Ordinary Differential Equation (ODE) solver to predict object trajectories. Unlike existing approaches that rely on discrete latent spaces, NFF captures fundamental physical concepts such as gravity, support, and collision in continuous explicit force fields. Experiments on three challenging physical reasoning tasks demonstrate that NFF, trained with only a few examples, achieves strong generalization to unseen scenarios. This physics-grounded representation enables efficient forward-backward planning and rapid adaptation through interactive refinement. Our work suggests that incorporating physics-inspired representations into learning systems can help bridge the gap between artificial and human physical reasoning capabilities.

1 Introduction

Physical reasoning, the ability to understand and predict how objects interact in the physical world, is fundamental to both human intelligence and artificial systems (Spelke, 2022). This capability underlies crucial applications ranging from robotics to scientific discovery, making it a central challenge in AI research (Lake et al., 2017). One of the remarkable aspects of human cognitive capabilities is the ability to rapidly learn from limited examples (Kim et al., 2020; Jiang et al., 2022; Lake and Baroni, 2023; Zhang et al., 2024), especially evident in intuitive physics (Kubricht et al., 2017; Bear et al., 2021). Humans can quickly abstract core physical principles after observing limited physical phenomena, enabling them to predict complex dynamics and interact with novel environments (Spelke and Kinzler, 2007; Battaglia et al., 2013; Bonawitz et al., 2019; Xu et al., 2021).

In contrast, current AI systems face significant limitations in physical reasoning. Despite being trained on gigantic datasets, these models still struggle to achieve human-level generalization, particularly in Out-of-distribution (OOD) settings (Lake et al., 2017; Zhu et al., 2020). The core issue lies in their tendency to overfit observed trajectories rather than capturing inherent physical principles, severely limiting their ability to compose known knowledge and predict outcomes in novel contexts (Qi et al., 2021; Li et al., 2022; Wu et al., 2023). This stark contrast between human capabilities and current model limitations has motivated the search for new approaches that can learn generalizable physical representations from minimal data.

Preprint. Under review.

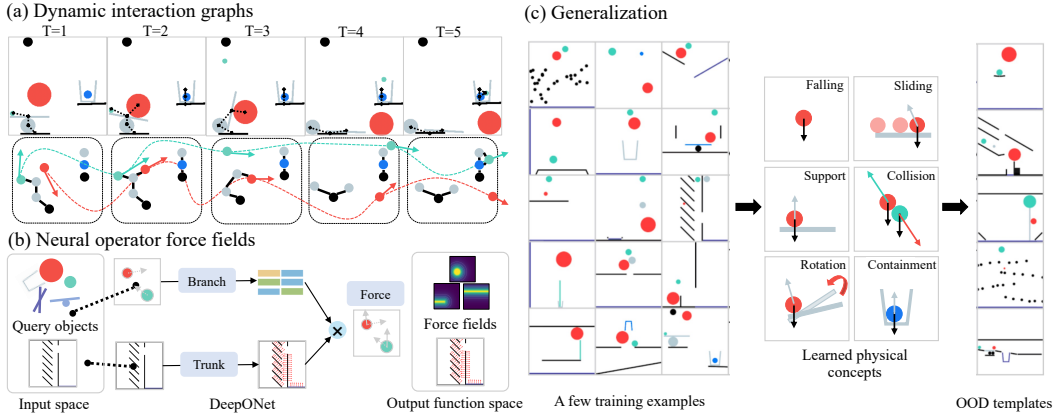


Figure 1: **The framework of NFF.** (a) NFF models complex physical interactions by constructing dynamic interaction graphs from scenes and performing continuous integration on force fields. (b) The force fields are inferred by a neural operator that takes object interactions as input. (c) After learning from a few examples, NFF can capture various physical concepts represented by force fields and generalize to unseen OOD scenarios.

To bridge this gap, we aim to develop agents with few-shot physical learning abilities that achieve robust generalization across diverse environments. This ambitious goal presents three fundamental challenges: (i) **Diverse Physical Dynamics:** Physical systems exhibit intricate and nonlinear dynamics shaped by complex object properties and interactions. OOD scenarios often present drastically different dynamics from training examples, requiring sophisticated representations that explicitly capture core physical principles. (ii) **Risk of Overfitting:** The few-shot learning setting dramatically increases the challenge of generalization compared to large-scale training approaches. Models must carefully balance between fitting observed examples and extracting broader physical principles. (iii) **Interactive Reasoning:** Effective physical reasoning demands more than passive observation—agents must actively engage with their environment through experimentation and feedback, adapting their understanding based on limited examples.

To address these challenges, we introduce Neural Force Field (NFF), a neural function map from objects to forces acting on continuous Euclidean coordinates for efficient interactive learning and reasoning. At its core, NFF employs a neural operator to learn dynamic force fields from external interventions and object interactions. These predicted forces are then integrated through an ODE solver to compute explicit physical variables such as velocity and displacement, producing interpretable results that align with established physical principles. Please refer to Fig. 1 for details.

Our framework offers three advantages. First, by representing physical interactions in low-dimensional neural operator force fields, NFF can rapidly learn fundamental physical concepts from just a few training examples. Second, due to the ODE-grounded dynamic graph, NFF can effectively generalize to OOD scenarios. Third, the integration of forces through an ODE solver enables fine-grained physical interactions, supporting precise modeling of collisions and gravity effects.

We evaluate our method using two state-based physical reasoning benchmarks—I-PHYRE (Li et al., 2023) and N-body problems (Newton, 1833)—as well as one vision-based benchmark, PHYRE (Bakhtin et al., 2019). These tasks feature complex rigid-body dynamics ranging from short-range forces (collision and sliding) to long-range forces (gravity). Our experiments demonstrate that NFF not only learns dynamics efficiently by abstracting physical interactions into force fields but also achieves strong generalization in both within-scenario and cross-scenario settings. Moreover, the framework’s physics-based representation enables effective forward and backward planning in goal-directed tasks, consistently outperforming existing methods such as Interaction Network (IN) (Battaglia et al., 2016; Qi et al., 2021) and transformer-based methods (Wu et al., 2023).

2 Related work

Physical reasoning Research in physical reasoning has progressed along two main trajectories: passive observation and interactive platforms. The passive observation approach, exemplified by the Violation-of-Expectation (VoE) paradigm (Spelke et al., 1992), evaluates physical understanding by measuring agents’ ability to detect violations of physics principles (Baillargeon, 1987; Hespos and

Baillargeon, 2001; Dai et al., 2023). While this approach has provided valuable insights into basic physical comprehension, it is limited in assessing active interventions and complex reasoning.

To enable more comprehensive evaluation, interactive platforms such as PHYRE (Bakhtin et al., 2019), the virtual tools game (Allen et al., 2020), and I-PHYRE (Li et al., 2023) have emerged. These environments require agents to actively manipulate objects to achieve specific goals, testing not only prediction capabilities but also planning and reasoning skills. However, existing approaches in these platforms often struggle with generalization across diverse scenarios, particularly in few-shot settings where limited training data is available (Qi et al., 2021; Li et al., 2023).

Current physical reasoning models face two primary challenges: the need for extensive training data and limited cross-scenario transferability. While some methods achieve strong performance within specific scenarios (Allen et al., 2020), they often fail to generalize their understanding to novel situations, falling short of human-level reasoning capabilities (Kang et al., 2024). Our work addresses these limitations by introducing a framework that unifies passive observation and interactive learning through dynamic **force fields**. The NFF approach enables few-shot learning of physical principles while supporting active reasoning through its interpretable force-based representation, facilitating both accurate prediction and effective intervention planning across diverse physical scenarios.

Dynamic prediction The prediction of physical dynamics, fundamental to intuitive physics, has evolved along two methodological branches: discrete and continuous-time approaches. Discrete methods typically combine recurrent architectures with GNNs (Battaglia et al., 2016; Qi et al., 2021) or transformer modules (Wu et al., 2023) for modeling object interactions, while leveraging convolutional operators for processing pixel-based information (Shi et al., 2015; Wang et al., 2022). Despite their flexibility in handling various interaction types, these methods often struggle with two key limitations: difficulty in extracting robust physical representations and susceptibility to error accumulation over extended time horizons.

Continuous-time methods address the above issues by incorporating physical inductive biases via explicit modeling of state derivatives within dynamical systems (Chen et al., 2018; Zhong et al., 2020; Norcliffe et al., 2020). While they improve long-term prediction, current systems typically assume energy-conservative systems with simplified dynamics (Greydanus et al., 2019; Cranmer et al., 2020) or static fields (Kofinas et al., 2023). More importantly, these methods face significant challenges in few-shot learning and struggle with cross-scenario generalization (Chen et al., 2020; Yuan et al., 2024), often requiring specific priors and grammars to achieve meaningful transfer (Xu et al., 2021). Although Physics-informed Neural Networks (PINN) can be precise in modeling physical dynamics, they depend heavily on prior knowledge of the underlying equations (Chu et al., 2022).

Our work advances continuous-time methods to model complex rigid body interactions via learnable dynamic **force fields**. This approach enables robust cross-scenario generalization while handling non-conservative energy systems. By combining the stability advantages of continuous-time modeling with flexible force field representations, NFF achieves both accurate long-term predictions and strong generalization capabilities without requiring explicit physical priors.

3 Method

3.1 The Neural Force Field (NFF) representation

Traditional approaches to modeling physical interactions typically rely on implicit representations through hidden vectors to describe object interactions. These methods use neural networks to learn state transition functions that map current scene features to future states. However, this purely data-driven approach cannot guarantee physically grounded representations, leading to poor generalization despite intensive training. We introduce NFF, which addresses these limitations by learning physics-grounded, generalizable representations through explicit force field modeling; see Fig. 2 for a comparison.

Predicting force field The core of NFF is built on the physical concept of a force field—a vector field that determines the force experienced by any query object based on its state \mathbf{z}^q . For a scene with N objects, we model the force field $\mathbf{F}(\cdot)$ at time t using a neural network operating on a relation graph \mathcal{G} . The graph contains object nodes $V = \{\mathbf{z}^0(t), \mathbf{z}^1(t), \dots, \mathbf{z}^{N-1}(t)\}$. Following neural operator methods (Lu et al., 2021) and graph neural models (Battaglia et al., 2018), we formulate

the force field function as:

$$\mathbf{F}(\mathbf{z}^q(t)) = \sum_{i \in \mathcal{G}(q)} \mathbf{W} (f_\theta(\mathbf{z}^i(t)) \odot f_\phi(\mathbf{z}^q(t))) + \mathbf{b}, \quad (1)$$

where $\mathcal{G}(q)$ represents the neighbors of query q determined by contacts or attractions, f_θ and f_ϕ are neural networks with parameters θ and ϕ , and $\mathbf{W} \in \mathbb{R}^{d_{\text{hidden}} \times d_{\text{force}}}$, $\mathbf{b} \in \mathbb{R}^{d_{\text{force}}}$ map hidden features to low-dimensional forces. The state vector \mathbf{z} incorporates zero-order (position, angle) and first-order (velocity, angular velocity) states. This representation can handle various physical interactions including collision, sliding, rotation, and gravity, as shown in Fig. 1.

Decoding trajectory with ODE Rather than relying on neural decoders, NFF employs a second-order ODE integrator to compute object trajectories from the learned force field. This approach ensures physically consistent trajectories governed by fundamental principles. The dynamic change of motion for a query state follow:

$$\frac{d^2 x^q(t)}{dt^2} = \frac{dv^q(t)}{dt} \propto \mathbf{F}(\mathbf{z}^q(t)). \quad (2)$$

While object mass theoretically affects acceleration, these mass constants are safely absorbed into the learned $F(\cdot)$ either by being explicitly included as inputs or implicitly captured through correlated physical attributes like size.

Solving ODEs We solve the ODE system using integration methods such as Runge-Kutta and Euler:

$$\mathbf{z}^q(t) = \text{ODESolve}(\mathbf{z}^q(0), \mathbf{F}, 0, t), \quad (3)$$

$$\begin{cases} \mathbf{x}(t) = \mathbf{x}(0) + \int_0^t \mathbf{v}(t) dt, \\ \mathbf{v}(t) = \mathbf{v}(0) + \int_0^t \mathbf{F}(\mathbf{z}^q(t)) dt, \end{cases} \quad (4)$$

The NFF framework offers three key advantages over existing approaches. First, it enables few-shot learning of force fields from minimal examples—even single trajectories—through its low-dimensional, physically-grounded representation $\mathbf{F}(\mathbf{z}^q(t))$, adhering to Eq. (2). Second, by representing interactions as neural operator force fields, as shown in Eq. (1), NFF can generalize the learned force patterns to novel scenarios through simple force summation on new interaction graphs, allowing modeling varying object compositions, interaction types, and time horizons. Third, the high-precision integration decoder, formulated in Eqs. (3) and (4), enables both fine-grained modeling of continuous-time interactions and efficient optimization for planning tasks through its invertible information flow. This precision supports various applications, from determining initial conditions for desired outcomes to designing targeted force fields for specific behaviors. The effectiveness of these three components—ODE grounding, Neural Operator Learning (NOL), and precise integration—is systematically validated through ablation studies in Sec. 4.5.

Training NFF The framework employs autoregressive prediction, using previously predicted states to generate current states. Network optimization minimizes the Mean Squared Error (MSE) loss between predictions and ground truth. To promote learning of local, generalizable dynamics rather than global patterns, we segment long trajectories into smaller units during training. This alleviates the issue of accumulated error in teacher forcing while reducing the complexity in recursive training. In evaluation, the model predicts all future dynamics given only the initial states.

3.2 Interactive planning

NFF extends beyond forward prediction to enable mental simulation for planning tasks. Given goal-directed scenarios, NFF can serve as a learned simulator to either search for action sequences that

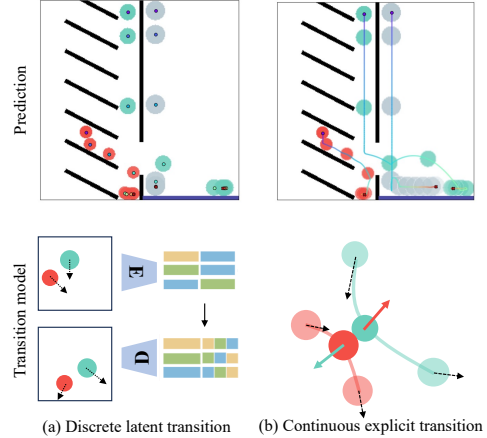


Figure 2: **Comparison between discrete latent transition in traditional interaction modeling and continuous explicit transition in NFF.** Traditional interaction models such as IN and SlotFormer decode discrete frames from a learnable decoder. In contrast, NFF decodes trajectories by integrating the continuous force using an ODE solver, which benefits learning detailed interactions such as collisions.

achieve the desired goal state through forward simulation, or optimize initial conditions and system parameters through backward computation.

Forward planning For physical reasoning tasks requiring specific action sequences, we extend the NFF framework to incorporate action effects by including action features in f_θ . Through forward simulation with the NFF model, we sample multiple action sequences $A = \{a_0, \dots, a_T\}$ and optimize according to evaluation metrics R : $A^* = \underset{A}{\operatorname{argmax}} R(\mathbf{F}, A)$. The optimal sequence A^* can

then be executed in the physical environment. While the forward simulation may initially deviate from actual observations, NFF’s physics-based design enables efficient adaptation through new experimental data, inspired by human trial-and-error learning (Allen et al., 2020). When executed trajectories deviate from the desired goal state, the new state sequences can be directly incorporated into model optimization through the MSE loss, following the same training procedure used in the initial learning.

Backward planning The invertible nature of the NFF formulation makes backward computation particularly efficient. By inverting the time direction of ODE integrator, NFF enables the inversion of initial conditions given a desired goal state: $\mathbf{x}(0) = \mathbf{x}(t) + \int_t^0 \mathbf{v}(t) dt$, $\mathbf{v}(0) = \mathbf{v}(t) + \int_t^0 \mathbf{F}(\mathbf{z}^g(t)) dt$, consistent with the learned physical dynamics encoded in the NFF model, as shown in Sec. 4.4.

4 Experiments

4.1 Environments and datasets

We evaluate state-based NFF on I-PHYRE and N-body dynamics and vision-based NFF on PHYRE. Each task is evaluated across three distinct settings: within-scenario prediction, cross-scenario prediction, and planning. Detailed environment and dataset configurations are provided in Appx. A.

I-PHYRE I-PHYRE (Li et al., 2023) presents a suite of complex physical reasoning puzzles requiring multi-step interventions. The environment incorporates diverse physical interactions including gravity, collision, friction, rotation, spring dynamics, and pendulum motion. It challenges AI agents to solve puzzles with minimal environmental interactions while generalizing to unseen scenarios. For within-scenario prediction, we evaluate on 10 training games that share similar scenarios but require different solutions. The cross-scenario prediction setting extends to 30 novel games featuring noise, compositional elements, and multi-ball scenarios, with varying object properties such as block lengths, ball sizes, and object positions. In the planning setting, models must generate optimal action sequences to successfully complete each game.

N-body The N-body problem (Newton, 1833) tests trajectory prediction for small comets orbiting a massive central planet. Using REBOUND simulator (Rein and Liu, 2012), we generate dynamics by randomly sampling orbital parameters including radii, angles, and masses. This task evaluates the model’s ability to infer gravitational laws from limited observations. The within-scenario prediction introduces novel initial conditions and masses, focusing on systems with 1-2 orbiting bodies tracked over 50 timesteps. Cross-scenario prediction significantly increases complexity by introducing systems with 7 or 9 orbiting bodies tracked over 150 timesteps. The planning setting challenges models to optimize initial conditions that will evolve to specified target states after 50 timesteps.

PHYRE Building on the previous two datasets that used state-based representations of objects, we explore extending NFF to a vision-based physical reasoning benchmark, PHYRE (Bakhtin et al., 2019). Designed for goal-oriented physical reasoning, PHYRE features 25 task templates involving interactive physics puzzles, all solvable by strategically placing a red ball. Each template generates 100 variations of a core task, supporting two distinct evaluation protocols: (i) the within-scenario setting, where models train on 80% of the tasks in each template and are tested on the remaining 20%; and (ii) the cross-scenario setting, which evaluates generalization by training on all tasks from 20 templates and testing on tasks from the 5 unseen ones.

4.2 Learning force fields from a few examples

We qualitatively evaluate NFF’s ability to inverse force fields **from limited observations** without direct access to ground-truth forces; training details are provided in Appx. B. For I-PHYRE, we train NFF on 10 basic games with 10 trajectory samples each. From these 100 trajectories, the model successfully learns fundamental physical concepts through unified force fields. To verify that

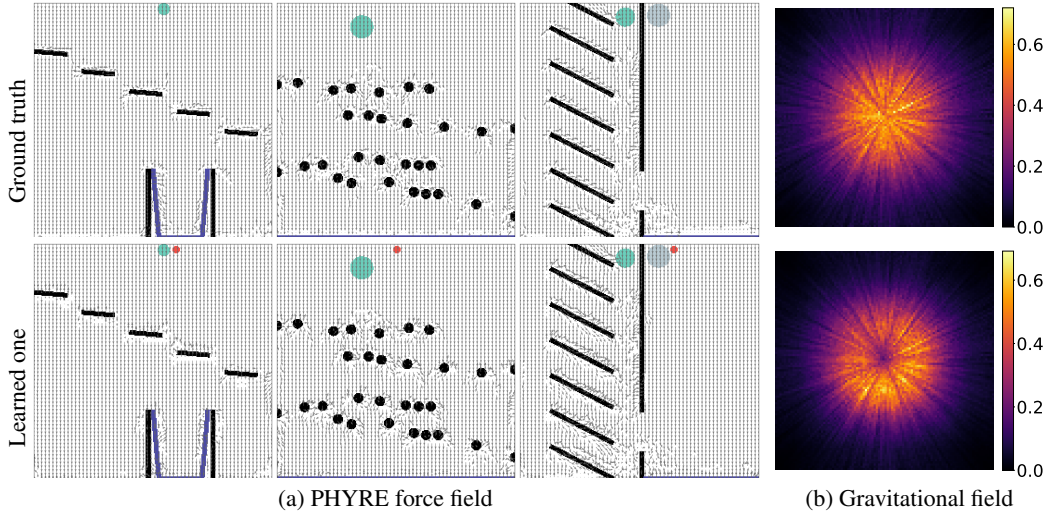


Figure 3: **Visualization of learned force fields after few-shot learning.** (a) NFF successfully inverts force fields across different templates on PHYRE, consisting of physical behaviors like falling under gravity, sliding with friction, and colliding with momentum transfer. (b) The learned gravitational field distributions in N-body also show accurate force field reconstruction.

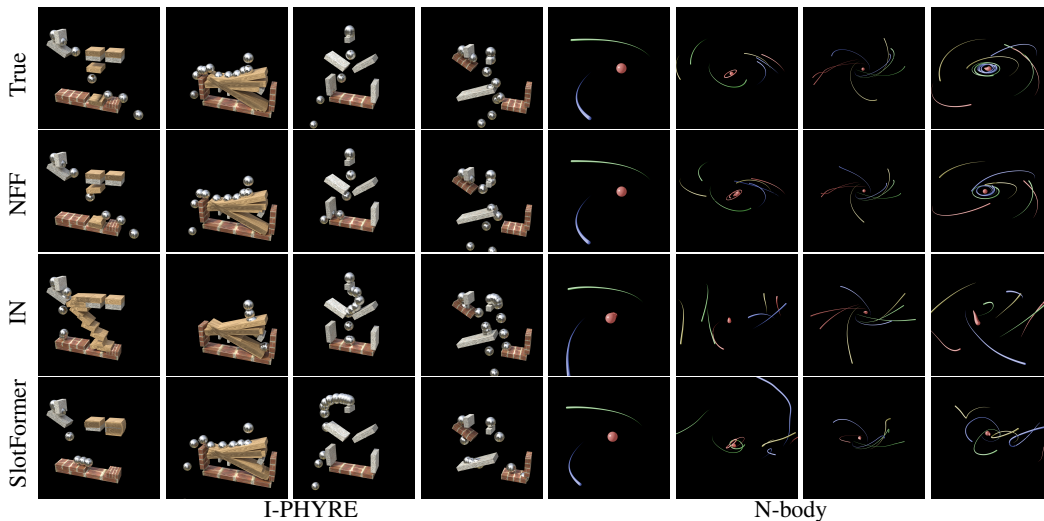


Figure 4: **Trajectory predictions on unseen scenarios after few-shot learning.** After learning from 100 and 200 trajectories on I-PHYRE and N-body systems, respectively, our NFF predictions closely match the ground truth behaviors across diverse scenarios, from rigid body interactions to gravitational dynamics. In contrast, other baselines fail to predict physically plausible dynamics. Additional visualizations are provided in [Appx. G](#).

NFF learns generalizable physical principles, we examine force responses to varied ball-block interactions under controlled conditions. [Fig. A1](#) shows our systematic evaluation where we independently vary individual parameters such as position, velocity, and angle while holding others constant, demonstrating NFF’s accurate force response modeling. For the N-body system, we train NFF using 200 randomly sampled trajectories from 2-body and 3-body dynamics. As shown in [Fig. 3b](#), the model successfully learns to capture the inverse gravitational field, correctly modeling the distance-dependent centripetal forces governing the mutual attraction between bodies. For PHYRE, we train a vision-based NFF on 12,000 trajectories (20 templates \times 20 tasks \times 30 actions), which is about 267 times less data than prior SOTA ([Qi et al., 2021](#)). As shown in [Fig. 3a](#), the model accurately captures force fields across diverse templates.

4.3 Prediction on unseen scenarios

We evaluate the learned force fields’ predictive accuracy in both within- and cross-scenario settings. For I-PHYRE, we test against 20 ground truth trajectories per game, while for N-body, we evaluate

Table 1: **NFF outperforms baselines on prediction tasks.** Comparison of NFF, IN (Battaglia et al., 2016), GCN (Kipf and Welling, 2016), and SlotFormer (Wu et al., 2023) on I-PHYRE and N-body tasks. Results are reported with Standard Error of the Mean (SEM); lower is better (\downarrow) for error metrics (RMSE, FPE, PCE), and higher is better (\uparrow) for correlation (R). NFF consistently yields lower errors and higher correlations, especially under cross-scenario generalization. The [0,3T] settings extend prediction from 50 to 150 steps.

Metric	Model	I-PHYRE		N-body		
		Within	Cross	Within [0,T]	Within [0,3T]	Cross [0,3T]
RMSE \downarrow	IN	0.124 \pm 0.007	0.194 \pm 0.004	0.306 \pm 0.022	0.832 \pm 0.034	4.727 \pm 0.111
	GCN	0.118 \pm 0.008	0.213 \pm 0.006	0.387 \pm 0.028	1.090 \pm 0.050	2.130 \pm 0.046
	Slotformer	0.067 \pm 0.006	0.206 \pm 0.005	0.257 \pm 0.021	1.117 \pm 0.042	3.531 \pm 0.128
	NFF	0.048 \pm 0.004	0.131 \pm 0.004	0.139 \pm 0.012	0.558 \pm 0.024	1.090 \pm 0.023
FPE \downarrow	IN	0.129 \pm 0.010	0.178 \pm 0.005	0.283 \pm 0.019	0.740 \pm 0.026	5.376 \pm 0.152
	GCN	0.118 \pm 0.009	0.213 \pm 0.006	0.332 \pm 0.023	1.028 \pm 0.048	2.147 \pm 0.046
	Slotformer	0.068 \pm 0.007	0.198 \pm 0.005	0.250 \pm 0.018	1.289 \pm 0.066	3.708 \pm 0.134
	NFF	0.042 \pm 0.004	0.111 \pm 0.004	0.147 \pm 0.013	0.506 \pm 0.022	1.166 \pm 0.024
PCE \downarrow	IN	0.004 \pm 0.000	0.005 \pm 0.000	0.018 \pm 0.002	0.034 \pm 0.003	0.060 \pm 0.002
	GCN	0.003 \pm 0.000	0.194 \pm 0.000	0.021 \pm 0.002	0.034 \pm 0.002	0.041 \pm 0.002
	Slotformer	0.002 \pm 0.000	0.004 \pm 0.000	0.015 \pm 0.002	0.039 \pm 0.002	0.075 \pm 0.002
	NFF	0.001 \pm 0.000	0.003 \pm 0.000	0.008 \pm 0.001	0.022 \pm 0.002	0.032 \pm 0.002
R \uparrow	IN	0.993 \pm 0.001	0.974 \pm 0.001	0.968 \pm 0.004	0.870 \pm 0.011	0.325 \pm 0.020
	GCN	0.991 \pm 0.001	0.969 \pm 0.002	0.956 \pm 0.005	0.834 \pm 0.013	0.586 \pm 0.023
	Slotformer	0.997 \pm 0.001	0.967 \pm 0.001	0.977 \pm 0.003	0.870 \pm 0.010	0.420 \pm 0.024
	NFF	0.997 \pm 0.001	0.980 \pm 0.002	0.992 \pm 0.001	0.938 \pm 0.007	0.826 \pm 0.011

using 200 unseen initial conditions. We compare against established interaction modeling methods: IN (Battaglia et al., 2016), GCN (Kipf and Welling, 2016), and SlotFormer (Wu et al., 2023).

Evaluation metrics We employ multiple complementary metrics to assess prediction quality. Beyond standard Root Mean Squared Error (RMSE), we introduce Final Position Error (FPE) and Position Change Error (PCE) for detailed performance analysis. FPE quantifies terminal position accuracy, while PCE evaluates the model’s ability to capture motion dynamics. Additionally, Pearson Correlation Coefficient (R) measures trajectory shape alignment independent of speed variations. This comprehensive metric suite enables thorough evaluation across temporal and spatial dimensions. Detailed definitions are provided in [Appx. B.2](#).

Results As shown in [Fig. 4](#), NFF generates physically plausible trajectories that closely match ground truth behavior, even in previously unseen scenarios. Quantitative results in [Tab. 1](#) demonstrate NFF’s superior performance across all metrics for both I-PHYRE and N-body tasks, with particularly strong results in cross-scenario generalization. While other models exhibit overfitting tendencies that limit the cross-scenario performance, NFF’s ability to learn generalizable physical principles enables robust prediction across diverse scenarios. Additional results in [Appx. D](#) demonstrate the superior robustness of our model under noisy state conditions.

4.4 Planning on unseen scenarios

The trained NFF model can generate plans for novel tasks after learning from limited demonstrations. Unlike prediction tasks that evaluate trajectory accuracy, planning tasks require generating action sequences to achieve specific goals.

I-PHYRE planning We implement a 5-round interactive learning protocol. NFF acts as a mental simulator to evaluate 500 randomly sampled action candidates (when to eliminate which block in order to drop the balls into the abyss), selecting the optimal sequence for physical execution. After each execution, the model updates its parameters based on observed outcomes, refining its physics understanding. This updated model then guides subsequent action proposals.

We quantitatively evaluate planning by calculating success probability p_i for each game as the success rate over 20 trials in round i , with NFF updating after failures; see detailed results in [Appx. F](#). [Figure 6](#) compares NFF against random sampling, human performance (from [Li et al. \(2023\)](#)), IN, and SlotFormer using cumulative success probability: $1 - \prod_{i=1}^n (1 - p_i)$ for current round n . NFF outperforms baselines and approaches human-level performance after refinement ([Allen et al.](#),

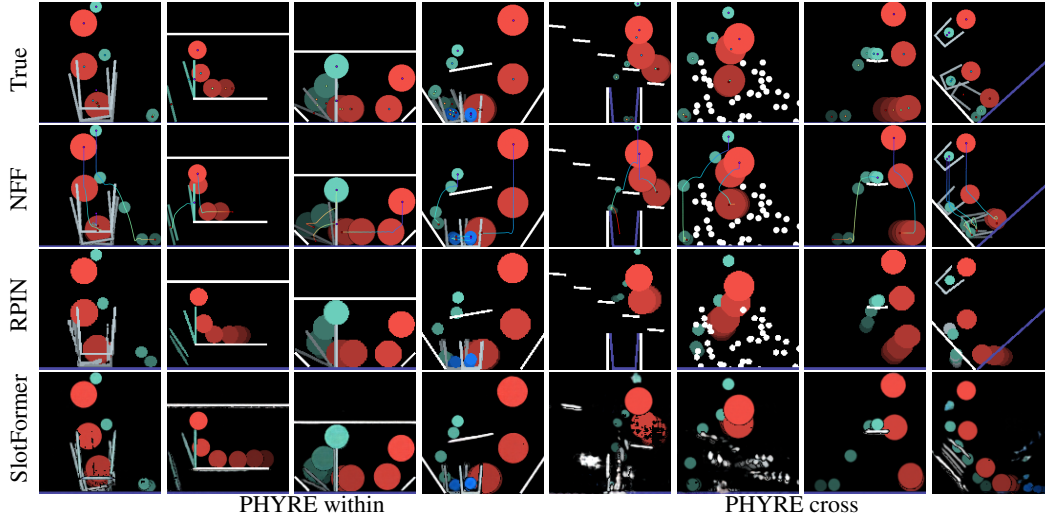


Figure 5: **Trajectory Predictions on PHYRE.** We compare the vision-based NFF, trained on 12,000 trajectories, with SOTA methods trained on 3.2 million trajectories. Prior methods decoding objects from latent spaces often suffer from object inconsistency. For example, in the last column, RPIN mistakenly transforms a gray cup into a gray ball, indicating overfitting to training shapes. SlotFormer also shows object disappearance in cross-scenario tasks. In contrast, NFF produces more accurate predictions while maintaining object consistency.

2020), demonstrating effective few-shot learning. The performance of IN and SlotFormer, falling below random sampling, indicates how inaccurate dynamics modeling compromises planning.

N-body planning We focus on determining initial conditions that achieve desired final configurations under celestial dynamics. NFF’s inverse simulation enables direct computation of initial conditions through reverse time evolution, while IN and SlotFormer rely on iterative gradient-based refinement. As shown in Tab. 2, NFF achieves superior planning performance in both within- and cross-scenario settings.

PHYRE planning In PHYRE, we extend NFF to learn dynamics directly from RGB videos with segmentation masks by applying sparse convolutions to extract geometric features from the masked objects. Following PHYRE’s standard evaluation protocol, we first utilize NFF to predict trajectories and then use a pretrained TimeSFormer (Bertasius et al., 2021) as the classifier to determine task success or failure. Planning performance is measured by the AUCESS metric (Bakhtin et al., 2019), which captures both effectiveness and efficiency by assigning higher weight to solutions that succeed with fewer attempts. Specifically, each attempt count $k \in 1, 2, 3, \dots, 100$ is weighted by $\omega_k = \log(k+1) - \log(k)$, and the final AUCESS score is computed as: $\frac{\sum_k \omega_k \cdot s_k}{\sum_k \omega_k}$, where s_k is the success rate within k attempts.

We compare NFF against the RPIN (Qi et al., 2021) and SlotFormer (Wu et al., 2023). As shown qualitatively in Fig. 5, NFF, trained on just 0.012 million trajectories, learns physically grounded dynamics that support effective planning while maintaining higher fidelity and stronger object permanence than RPIN and SlotFormer, particularly in cross-scenario generalization. Quantitative results in Tab. 3 further demonstrate that NFF outperforms state-of-the-art baselines in the challenging cross-scenario tasks. In contrast, SlotFormer’s slot attention leads to limited generalization in unseen objects, resulting in planning failures in cross scenarios; see Fig. A6 for more analysis.

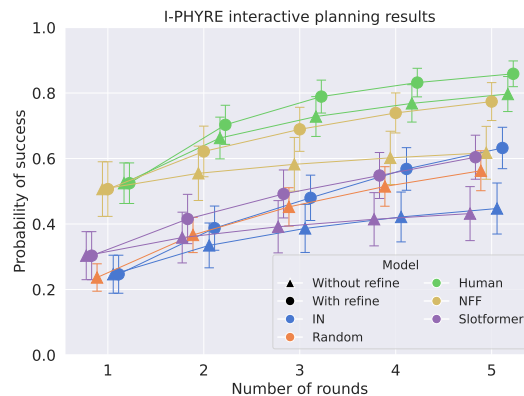


Figure 6: **Interactive planning performance on I-PHYRE.** Comparison of cumulative success probability over 5 planning rounds among human, random sampling, our NFF, IN, and SlotFormer. Error bars show SEM across trials. Our NFF with refinement (Allen et al., 2020) shows continuous improvement across rounds, achieving performance comparable to human (data from Li et al. (2023)), while others show limited performance even with refinement.

Table 2: **N-body system initial condition reconstruction from target configurations.** Results show average MSE \downarrow with SEM across trials for both within- and cross-scenario evaluations.

Scenario	IN	SlotFormer	NFF
Within \downarrow	0.651 ± 0.021	0.837 ± 0.029	0.067 ± 0.010
Cross \downarrow	4.654 ± 0.193	4.018 ± 0.133	0.140 ± 0.011

Table 3: **Planning performance on PHYRE in the cross-scenario setting.** Training sample size (in millions) and AUCESS \uparrow score are reported. Our NFF achieves the best performance with the least data.

Metric	DQN	RPIN	SlotFormer	NFF
Sample (M)	200.000	3.200	0.120	0.012
AUCESS	30.96	36.58	21.04	49.22

Table 4: **Ablation results emphasize the need for high integration precision, ODE grounding, and NOL.** We test NFF with different integration precision. The NFF without ODE grounding degenerates to IN with the same integration precision ($1e-3$) and the NFF without NOL utilize an MLP as force predictor instead of DeepONet. NFF with high integration precision, ODE, and NOL yields the best generalization results.

Scenario	NFF $1e-3$	NFF $5e-3$	NFF $1e-2$	NFF $5e-2$	w/o ODE	w/o NOL
Training	0.083 ± 0.009	0.137 ± 0.014	0.129 ± 0.016	0.231 ± 0.022	0.044 ± 0.005	0.056 ± 0.005
Within	0.095 ± 0.008	0.139 ± 0.013	0.136 ± 0.014	0.239 ± 0.020	0.354 ± 0.023	0.120 ± 0.021
Within [0,3T]	0.471 ± 0.025	0.558 ± 0.024	0.535 ± 0.027	0.693 ± 0.030	0.949 ± 0.041	0.540 ± 0.042
Cross	1.024 ± 0.021	1.090 ± 0.023	1.084 ± 0.024	1.315 ± 0.033	3.518 ± 0.061	1.347 ± 0.128

4.5 Ablation study

We investigate three key factors that may affect NFF performance, including integration precision, ODE grounding, and NOL. For **integration precision**, we evaluate NFF on the N-body task using Euler integration at four precision levels: $1e-3$, $5e-3$, $1e-2$, and $5e-2$. **Tab. 4** demonstrates that higher integration precision consistently yields better performance. We also explore more integration methods in **Appx. C**. To study **ODE grounding**'s impact on generalization, we compare two configurations: our NFF using predicted force fields with ODE integration, and IN using learned state transitions at matching step sizes. **Tab. 4** shows that ODE integration enhances generalization performance. For **NOL**, we replace the DeepONet in NFF with a vanilla MLP. The results in the last column of **Tab. 4** show a consistent increase in generalization errors across settings compared with NFF with DeepONet (column one). These ablation studies demonstrate that NFF achieves optimal few-shot learning of physical dynamics when combining high integration precision, ODE-based integration, and NOL.

5 Discussion

Modeling diverse forces While NFF has demonstrated effectiveness in modeling fundamental physical forces like gravity, support, and collision, its principles extend naturally to broader domains. The framework can potentially model social forces (Shu et al., 2015; Xie et al., 2017; Wei et al., 2017, 2018; Shu et al., 2021) and biological forces governing migration patterns and human motion (Netanyahu et al., 2024). **Limitations** While our experiments focus on generalization across varying object masses, training a single model with varying friction and elasticity may pose additional challenges. Furthermore, for a clear and constrained validation of learning forces, we assume a deterministic environment with rigid bodies and have not explored the model's performance in stochastic environments or those containing soft bodies and fluids. **Impact statements** The proposed NFF framework could enable more sample-efficient and interpretable physical modeling, reducing data needed for training. We acknowledge potential risks if misused for simulating harmful physical scenarios. However, the research focuses on basic physical principles and publicly available phenomena, prioritizing transparent and reproducible science.

6 Conclusion

We present NFF, a force field-based representation framework for modeling complex physical interactions that exhibits human-like few-shot learning, generalization, and reasoning capabilities. Our experiments on three challenging physical reasoning datasets demonstrate NFF's ability to not only learn diverse physical concepts and rules from limited observations but also generalize to unseen scenarios for both prediction and planning tasks. This initial exploration of the force field may provide new perspectives for developing physical world models through representation learning, potentially bridging the gap between human physical understanding and learning-based methods.

Acknowledgements

The authors would like to thank Miss Chen Zhen (BIGAI) for making the nice figures, Prof. Yizhou Wang (Peking University) for the helpful discussion, and Minyang Yu (Peking University) for working on the GPT’s results. This work is supported in part by the National Natural Science Foundation of China (62376031), the State Key Lab of General AI at Peking University, the PKU-BingJi Joint Laboratory for Artificial Intelligence, and the National Comprehensive Experimental Base for Governance of Intelligent Society, Wuhan East Lake High-Tech Development Zone.

References

- Allen, K. R., Smith, K. A., and Tenenbaum, J. B. (2020). Rapid trial-and-error learning with simulation supports flexible tool use and physical reasoning. *Proceedings of the National Academy of Sciences (PNAS)*, 117(47):29302–29310. 3, 5, 7, 8
- Baillargeon, R. (1987). Object permanence in 31 2- and 41 2-month-old infants. *Developmental Psychology*, 23(5):655–664. 2
- Bakhtin, A., van der Maaten, L., Johnson, J., Gustafson, L., and Girshick, R. (2019). Phyre: A new benchmark for physical reasoning. In *Proceedings of Advances in Neural Information Processing Systems (NeurIPS)*. 2, 3, 5, 8
- Battaglia, P., Pascanu, R., Lai, M., Jimenez Rezende, D., et al. (2016). Interaction networks for learning about objects, relations and physics. In *Proceedings of Advances in Neural Information Processing Systems (NeurIPS)*. 2, 3, 7
- Battaglia, P. W., Hamrick, J. B., Bapst, V., Sanchez-Gonzalez, A., Zambaldi, V., Malinowski, M., Tacchetti, A., Raposo, D., Santoro, A., Faulkner, R., et al. (2018). Relational inductive biases, deep learning, and graph networks. *arXiv preprint arXiv:1806.01261*. 3
- Battaglia, P. W., Hamrick, J. B., and Tenenbaum, J. B. (2013). Simulation as an engine of physical scene understanding. *Proceedings of the National Academy of Sciences (PNAS)*. 1
- Bear, D. M., Wang, E., Mrowca, D., Binder, F. J., Tung, H.-Y. F., Pramod, R., Holdaway, C., Tao, S., Smith, K., Sun, F.-Y., et al. (2021). Physion: Evaluating physical prediction from vision in humans and machines. In *Proceedings of Advances in Neural Information Processing Systems (NeurIPS)*. 1
- Bertasius, G., Wang, H., and Torresani, L. (2021). Is space-time attention all you need for video understanding? In *Proceedings of International Conference on Machine Learning (ICML)*. 8
- Bonawitz, E., Ullman, T. D., Bridgers, S., Gopnik, A., and Tenenbaum, J. B. (2019). Sticking to the evidence? a behavioral and computational case study of micro-theory change in the domain of magnetism. *Cognitive science*, 43(8):e12765. 1
- Chen, R. T., Amos, B., and Nickel, M. (2020). Learning neural event functions for ordinary differential equations. *arXiv preprint arXiv:2011.03902*. 3
- Chen, R. T., Rubanova, Y., Bettencourt, J., and Duvenaud, D. K. (2018). Neural ordinary differential equations. In *Proceedings of Advances in Neural Information Processing Systems (NeurIPS)*. 3
- Chu, M., Liu, L., Zheng, Q., Franz, E., Seidel, H.-P., Theobalt, C., and Zayer, R. (2022). Physics informed neural fields for smoke reconstruction with sparse data. *ACM Transactions on Graphics (ToG)*, 41(4):1–14. 3
- Cranmer, M., Greydanus, S., Hoyer, S., Battaglia, P., Spergel, D., and Ho, S. (2020). Lagrangian neural networks. In *ICLR Workshop on Integration of Deep Neural Models and Differential Equations*. 3
- Dai, B., Wang, L., Jia, B., Zhang, Z., Zhu, S.-C., Zhang, C., and Zhu, Y. (2023). X-voe: Measuring explanatory violation of expectation in physical events. In *Proceedings of International Conference on Computer Vision (ICCV)*. 3
- Greydanus, S., Dzamba, M., and Yosinski, J. (2019). Hamiltonian neural networks. In *Proceedings of Advances in Neural Information Processing Systems (NeurIPS)*. 3
- Hespos, S. J. and Baillargeon, R. (2001). Infants’ knowledge about occlusion and containment events: A surprising discrepancy. *Psychological Science*, 12(2):141–147. 2

- Jiang, H., Ma, X., Nie, W., Yu, Z., Zhu, Y., and Anandkumar, A. (2022). Bongard-hoi: Benchmarking few-shot visual reasoning for human-object interactions. In *Proceedings of Conference on Computer Vision and Pattern Recognition (CVPR)*. 1
- Kang, B., Yue, Y., Lu, R., Lin, Z., Zhao, Y., Wang, K., Huang, G., and Feng, J. (2024). How far is video generation from world model: A physical law perspective. *arXiv preprint arXiv:2411.02385*. 3
- Kim, Y., Shin, J., Yang, E., and Hwang, S. J. (2020). Few-shot visual reasoning with meta-analogical contrastive learning. In *Proceedings of Advances in Neural Information Processing Systems (NeurIPS)*. 1
- Kipf, T. N. and Welling, M. (2016). Semi-supervised classification with graph convolutional networks. *arXiv preprint arXiv:1609.02907*. 7
- Kofinas, M. M., Bekkers, E., Nagaraja, N., and Gavves, E. (2023). Latent field discovery in interacting dynamical systems with neural fields. In *Proceedings of Advances in Neural Information Processing Systems (NeurIPS)*. 3
- Kubricht, J. R., Holyoak, K. J., and Lu, H. (2017). Intuitive physics: Current research and controversies. *Trends in Cognitive Sciences*, 21(10):749–759. 1
- Lake, B. M. and Baroni, M. (2023). Human-like systematic generalization through a meta-learning neural network. *Nature*, 623(7985):115–121. 1
- Lake, B. M., Ullman, T. D., Tenenbaum, J. B., and Gershman, S. J. (2017). Building machines that learn and think like people. *Behavioral and brain sciences*, 40:e253. 1
- Li, S., Wu, K., Zhang, C., and Zhu, Y. (2022). On the learning mechanisms in physical reasoning. In *Proceedings of Advances in Neural Information Processing Systems (NeurIPS)*. 1
- Li, S., Wu, K., Zhang, C., and Zhu, Y. (2023). I-phyre: Interactive physical reasoning. In *Proceedings of International Conference on Learning Representations (ICLR)*. 2, 3, 5, 7, 8, A1
- Lu, L., Jin, P., Pang, G., Zhang, Z., and Karniadakis, G. E. (2021). Learning nonlinear operators via deeponet based on the universal approximation theorem of operators. *Nature Machine Intelligence*, 3(3):218–229. 3
- Netanyahu, A., Du, Y., Bronars, A., Pari, J., Tenenbaum, J., Shu, T., and Agrawal, P. (2024). Few-shot task learning through inverse generative modeling. In *Proceedings of Advances in Neural Information Processing Systems (NeurIPS)*. 9
- Newton, I. (1833). *Philosophiae naturalis principia mathematica*, volume 1. G. Brookman. 2, 5
- Norcliffe, A., Bodnar, C., Day, B., Simidjievski, N., and Liò, P. (2020). On second order behaviour in augmented neural odes. In *Proceedings of Advances in Neural Information Processing Systems (NeurIPS)*. 3
- Qi, H., Wang, X., Pathak, D., Ma, Y., and Malik, J. (2021). Learning long-term visual dynamics with region proposal interaction networks. In *Proceedings of International Conference on Learning Representations (ICLR)*. 1, 2, 3, 6, 8
- Rein, H. and Liu, S.-F. (2012). Rebound: an open-source multi-purpose n-body code for collisional dynamics. *Astronomy & Astrophysics*, 537:A128. 5
- Shi, X., Chen, Z., Wang, H., Yeung, D.-Y., Wong, W.-K., and Woo, W.-c. (2015). Convolutional lstm network: A machine learning approach for precipitation nowcasting. In *Proceedings of Advances in Neural Information Processing Systems (NeurIPS)*. 3
- Shu, T., Peng, Y., Zhu, S.-C., and Lu, H. (2021). A unified psychological space for human perception of physical and social events. *Cognitive Psychology*, 128:101398. 9
- Shu, T., Xie, D., Rothrock, B., Todorovic, S., and Chun Zhu, S. (2015). Joint inference of groups, events and human roles in aerial videos. In *Proceedings of Conference on Computer Vision and Pattern Recognition (CVPR)*. 9
- Spelke, E. (2022). *What babies know: Core Knowledge and Composition volume 1*, volume 1. Oxford University Press. 1
- Spelke, E. S., Breinlinger, K., Macomber, J., and Jacobson, K. (1992). Origins of knowledge. *Psychological Review*, 99(4):605. 2

- Spelke, E. S. and Kinzler, K. D. (2007). Core knowledge. *Developmental Science*, 10(1):89–96. [1](#)
- Wang, Y., Wu, H., Zhang, J., Gao, Z., Wang, J., Philip, S. Y., and Long, M. (2022). Predrnn: A recurrent neural network for spatiotemporal predictive learning. *Transactions on Pattern Analysis and Machine Intelligence (TPAMI)*, 45(2):2208–2225. [3](#)
- Wei, P., Liu, Y., Shu, T., Zheng, N., and Zhu, S.-C. (2018). Where and why are they looking? jointly inferring human attention and intentions in complex tasks. In *Proceedings of Conference on Computer Vision and Pattern Recognition (CVPR)*. [9](#)
- Wei, P., Xie, D., Zheng, N., Zhu, S.-C., et al. (2017). Inferring human attention by learning latent intentions. In *International Joint Conference on Artificial Intelligence (IJCAI)*. [9](#)
- Wu, Z., Dvornik, N., Greff, K., Kipf, T., and Garg, A. (2023). Slotformer: Unsupervised visual dynamics simulation with object-centric models. In *Proceedings of International Conference on Learning Representations (ICLR)*. [1](#), [2](#), [3](#), [7](#), [8](#)
- Xie, D., Shu, T., Todorovic, S., and Zhu, S.-C. (2017). Learning and inferring “dark matter” and predicting human intents and trajectories in videos. *Transactions on Pattern Analysis and Machine Intelligence (TPAMI)*, 40(7):1639–1652. [9](#)
- Xu, K., Srivastava, A., Gutfreund, D., Sosa, F., Ullman, T., Tenenbaum, J., and Sutton, C. (2021). A bayesian-symbolic approach to reasoning and learning in intuitive physics. In *Proceedings of Advances in Neural Information Processing Systems (NeurIPS)*. [1](#), [3](#)
- Yuan, J., Sun, G., Xiao, Z., Zhou, H., Luo, X., Luo, J., Zhao, Y., Ju, W., and Zhang, M. (2024). Egode: An event-attended graph ode framework for modeling rigid dynamics. In *Proceedings of Advances in Neural Information Processing Systems (NeurIPS)*. [3](#)
- Zhang, C., Jia, B., Zhu, Y., and Zhu, S.-C. (2024). Human-level few-shot concept induction through minimax entropy learning. *Science Advances*, 10(16):eadg2488. [1](#)
- Zhong, Y. D., Dey, B., and Chakraborty, A. (2020). Symplectic ode-net: Learning hamiltonian dynamics with control. In *Proceedings of International Conference on Learning Representations (ICLR)*. [3](#)
- Zhu, Y., Gao, T., Fan, L., Huang, S., Edmonds, M., Liu, H., Gao, F., Zhang, C., Qi, S., Wu, Y. N., et al. (2020). Dark, beyond deep: A paradigm shift to cognitive ai with humanlike common sense. *Engineering*, 6(3):310–345. [1](#)

NeurIPS Paper Checklist

1. Claims

Question: Do the main claims made in the abstract and introduction accurately reflect the paper's contributions and scope?

Answer: [Yes]

Justification: We have illustrated the motivation and contribution of studying few-shot learning of generalizable physical reasoning in our abstract and introduction.

Guidelines:

- The answer NA means that the abstract and introduction do not include the claims made in the paper.
- The abstract and/or introduction should clearly state the claims made, including the contributions made in the paper and important assumptions and limitations. A No or NA answer to this question will not be perceived well by the reviewers.
- The claims made should match theoretical and experimental results, and reflect how much the results can be expected to generalize to other settings.
- It is fine to include aspirational goals as motivation as long as it is clear that these goals are not attained by the paper.

2. Limitations

Question: Does the paper discuss the limitations of the work performed by the authors?

Answer: [Yes]

Justification: See [Sec. 5](#).

Guidelines:

- The answer NA means that the paper has no limitation while the answer No means that the paper has limitations, but those are not discussed in the paper.
- The authors are encouraged to create a separate "Limitations" section in their paper.
- The paper should point out any strong assumptions and how robust the results are to violations of these assumptions (e.g., independence assumptions, noiseless settings, model well-specification, asymptotic approximations only holding locally). The authors should reflect on how these assumptions might be violated in practice and what the implications would be.
- The authors should reflect on the scope of the claims made, e.g., if the approach was only tested on a few datasets or with a few runs. In general, empirical results often depend on implicit assumptions, which should be articulated.
- The authors should reflect on the factors that influence the performance of the approach. For example, a facial recognition algorithm may perform poorly when image resolution is low or images are taken in low lighting. Or a speech-to-text system might not be used reliably to provide closed captions for online lectures because it fails to handle technical jargon.
- The authors should discuss the computational efficiency of the proposed algorithms and how they scale with dataset size.
- If applicable, the authors should discuss possible limitations of their approach to address problems of privacy and fairness.
- While the authors might fear that complete honesty about limitations might be used by reviewers as grounds for rejection, a worse outcome might be that reviewers discover limitations that aren't acknowledged in the paper. The authors should use their best judgment and recognize that individual actions in favor of transparency play an important role in developing norms that preserve the integrity of the community. Reviewers will be specifically instructed to not penalize honesty concerning limitations.

3. Theory assumptions and proofs

Question: For each theoretical result, does the paper provide the full set of assumptions and a complete (and correct) proof?

Answer: [NA]

Justification: [NA]

Guidelines:

- The answer NA means that the paper does not include theoretical results.
- All the theorems, formulas, and proofs in the paper should be numbered and cross-referenced.
- All assumptions should be clearly stated or referenced in the statement of any theorems.
- The proofs can either appear in the main paper or the supplemental material, but if they appear in the supplemental material, the authors are encouraged to provide a short proof sketch to provide intuition.
- Inversely, any informal proof provided in the core of the paper should be complemented by formal proofs provided in appendix or supplemental material.
- Theorems and Lemmas that the proof relies upon should be properly referenced.

4. Experimental result reproducibility

Question: Does the paper fully disclose all the information needed to reproduce the main experimental results of the paper to the extent that it affects the main claims and/or conclusions of the paper (regardless of whether the code and data are provided or not)?

Answer: [Yes]

Justification: See [Appx. B](#).

Guidelines:

- The answer NA means that the paper does not include experiments.
- If the paper includes experiments, a No answer to this question will not be perceived well by the reviewers: Making the paper reproducible is important, regardless of whether the code and data are provided or not.
- If the contribution is a dataset and/or model, the authors should describe the steps taken to make their results reproducible or verifiable.
- Depending on the contribution, reproducibility can be accomplished in various ways. For example, if the contribution is a novel architecture, describing the architecture fully might suffice, or if the contribution is a specific model and empirical evaluation, it may be necessary to either make it possible for others to replicate the model with the same dataset, or provide access to the model. In general, releasing code and data is often one good way to accomplish this, but reproducibility can also be provided via detailed instructions for how to replicate the results, access to a hosted model (e.g., in the case of a large language model), releasing of a model checkpoint, or other means that are appropriate to the research performed.
- While NeurIPS does not require releasing code, the conference does require all submissions to provide some reasonable avenue for reproducibility, which may depend on the nature of the contribution. For example
 - (a) If the contribution is primarily a new algorithm, the paper should make it clear how to reproduce that algorithm.
 - (b) If the contribution is primarily a new model architecture, the paper should describe the architecture clearly and fully.
 - (c) If the contribution is a new model (e.g., a large language model), then there should either be a way to access this model for reproducing the results or a way to reproduce the model (e.g., with an open-source dataset or instructions for how to construct the dataset).
 - (d) We recognize that reproducibility may be tricky in some cases, in which case authors are welcome to describe the particular way they provide for reproducibility. In the case of closed-source models, it may be that access to the model is limited in some way (e.g., to registered users), but it should be possible for other researchers to have some path to reproducing or verifying the results.

5. Open access to data and code

Question: Does the paper provide open access to the data and code, with sufficient instructions to faithfully reproduce the main experimental results, as described in supplemental material?

Answer: [Yes]

Justification: The data and code will be released after publication.

Guidelines:

- The answer NA means that paper does not include experiments requiring code.
- Please see the NeurIPS code and data submission guidelines (<https://nips.cc/public/guides/CodeSubmissionPolicy>) for more details.
- While we encourage the release of code and data, we understand that this might not be possible, so “No” is an acceptable answer. Papers cannot be rejected simply for not including code, unless this is central to the contribution (e.g., for a new open-source benchmark).
- The instructions should contain the exact command and environment needed to run to reproduce the results. See the NeurIPS code and data submission guidelines (<https://nips.cc/public/guides/CodeSubmissionPolicy>) for more details.
- The authors should provide instructions on data access and preparation, including how to access the raw data, preprocessed data, intermediate data, and generated data, etc.
- The authors should provide scripts to reproduce all experimental results for the new proposed method and baselines. If only a subset of experiments are reproducible, they should state which ones are omitted from the script and why.
- At submission time, to preserve anonymity, the authors should release anonymized versions (if applicable).
- Providing as much information as possible in supplemental material (appended to the paper) is recommended, but including URLs to data and code is permitted.

6. Experimental setting/details

Question: Does the paper specify all the training and test details (e.g., data splits, hyper-parameters, how they were chosen, type of optimizer, etc.) necessary to understand the results?

Answer: [Yes]

Justification: See [Appx. B](#).

Guidelines:

- The answer NA means that the paper does not include experiments.
- The experimental setting should be presented in the core of the paper to a level of detail that is necessary to appreciate the results and make sense of them.
- The full details can be provided either with the code, in appendix, or as supplemental material.

7. Experiment statistical significance

Question: Does the paper report error bars suitably and correctly defined or other appropriate information about the statistical significance of the experiments?

Answer: [Yes]

Justification: See [Sec. 4.3](#) and [Sec. 4.4](#).

Guidelines:

- The answer NA means that the paper does not include experiments.
- The authors should answer "Yes" if the results are accompanied by error bars, confidence intervals, or statistical significance tests, at least for the experiments that support the main claims of the paper.
- The factors of variability that the error bars are capturing should be clearly stated (for example, train/test split, initialization, random drawing of some parameter, or overall run with given experimental conditions).
- The method for calculating the error bars should be explained (closed form formula, call to a library function, bootstrap, etc.)
- The assumptions made should be given (e.g., Normally distributed errors).
- It should be clear whether the error bar is the standard deviation or the standard error of the mean.

- It is OK to report 1-sigma error bars, but one should state it. The authors should preferably report a 2-sigma error bar than state that they have a 96% CI, if the hypothesis of Normality of errors is not verified.
- For asymmetric distributions, the authors should be careful not to show in tables or figures symmetric error bars that would yield results that are out of range (e.g. negative error rates).
- If error bars are reported in tables or plots, The authors should explain in the text how they were calculated and reference the corresponding figures or tables in the text.

8. Experiments compute resources

Question: For each experiment, does the paper provide sufficient information on the computer resources (type of compute workers, memory, time of execution) needed to reproduce the experiments?

Answer: [Yes]

Justification: See [Appx. B](#).

Guidelines:

- The answer NA means that the paper does not include experiments.
- The paper should indicate the type of compute workers CPU or GPU, internal cluster, or cloud provider, including relevant memory and storage.
- The paper should provide the amount of compute required for each of the individual experimental runs as well as estimate the total compute.
- The paper should disclose whether the full research project required more compute than the experiments reported in the paper (e.g., preliminary or failed experiments that didn't make it into the paper).

9. Code of ethics

Question: Does the research conducted in the paper conform, in every respect, with the NeurIPS Code of Ethics <https://neurips.cc/public/EthicsGuidelines?>

Answer: [Yes]

Justification: We adhere to the NeurIPS Code of Ethics.

Guidelines:

- The answer NA means that the authors have not reviewed the NeurIPS Code of Ethics.
- If the authors answer No, they should explain the special circumstances that require a deviation from the Code of Ethics.
- The authors should make sure to preserve anonymity (e.g., if there is a special consideration due to laws or regulations in their jurisdiction).

10. Broader impacts

Question: Does the paper discuss both potential positive societal impacts and negative societal impacts of the work performed?

Answer: [Yes]

Justification: See [Sec. 5](#).

Guidelines:

- The answer NA means that there is no societal impact of the work performed.
- If the authors answer NA or No, they should explain why their work has no societal impact or why the paper does not address societal impact.
- Examples of negative societal impacts include potential malicious or unintended uses (e.g., disinformation, generating fake profiles, surveillance), fairness considerations (e.g., deployment of technologies that could make decisions that unfairly impact specific groups), privacy considerations, and security considerations.
- The conference expects that many papers will be foundational research and not tied to particular applications, let alone deployments. However, if there is a direct path to any negative applications, the authors should point it out. For example, it is legitimate to point out that an improvement in the quality of generative models could be used to

generate deepfakes for disinformation. On the other hand, it is not needed to point out that a generic algorithm for optimizing neural networks could enable people to train models that generate Deepfakes faster.

- The authors should consider possible harms that could arise when the technology is being used as intended and functioning correctly, harms that could arise when the technology is being used as intended but gives incorrect results, and harms following from (intentional or unintentional) misuse of the technology.
- If there are negative societal impacts, the authors could also discuss possible mitigation strategies (e.g., gated release of models, providing defenses in addition to attacks, mechanisms for monitoring misuse, mechanisms to monitor how a system learns from feedback over time, improving the efficiency and accessibility of ML).

11. Safeguards

Question: Does the paper describe safeguards that have been put in place for responsible release of data or models that have a high risk for misuse (e.g., pretrained language models, image generators, or scraped datasets)?

Answer: [NA]

Justification: [NA]

Guidelines:

- The answer NA means that the paper poses no such risks.
- Released models that have a high risk for misuse or dual-use should be released with necessary safeguards to allow for controlled use of the model, for example by requiring that users adhere to usage guidelines or restrictions to access the model or implementing safety filters.
- Datasets that have been scraped from the Internet could pose safety risks. The authors should describe how they avoided releasing unsafe images.
- We recognize that providing effective safeguards is challenging, and many papers do not require this, but we encourage authors to take this into account and make a best faith effort.

12. Licenses for existing assets

Question: Are the creators or original owners of assets (e.g., code, data, models), used in the paper, properly credited and are the license and terms of use explicitly mentioned and properly respected?

Answer: [Yes]

Justification: We have cited the baselines used in our experiments.

Guidelines:

- The answer NA means that the paper does not use existing assets.
- The authors should cite the original paper that produced the code package or dataset.
- The authors should state which version of the asset is used and, if possible, include a URL.
- The name of the license (e.g., CC-BY 4.0) should be included for each asset.
- For scraped data from a particular source (e.g., website), the copyright and terms of service of that source should be provided.
- If assets are released, the license, copyright information, and terms of use in the package should be provided. For popular datasets, paperswithcode.com/datasets has curated licenses for some datasets. Their licensing guide can help determine the license of a dataset.
- For existing datasets that are re-packaged, both the original license and the license of the derived asset (if it has changed) should be provided.
- If this information is not available online, the authors are encouraged to reach out to the asset's creators.

13. New assets

Question: Are new assets introduced in the paper well documented and is the documentation provided alongside the assets?

Answer: [NA]

Justification: [NA]

Guidelines:

- The answer NA means that the paper does not release new assets.
- Researchers should communicate the details of the dataset/code/model as part of their submissions via structured templates. This includes details about training, license, limitations, etc.
- The paper should discuss whether and how consent was obtained from people whose asset is used.
- At submission time, remember to anonymize your assets (if applicable). You can either create an anonymized URL or include an anonymized zip file.

14. **Crowdsourcing and research with human subjects**

Question: For crowdsourcing experiments and research with human subjects, does the paper include the full text of instructions given to participants and screenshots, if applicable, as well as details about compensation (if any)?

Answer: [NA]

Justification: [NA]

Guidelines:

- The answer NA means that the paper does not involve crowdsourcing nor research with human subjects.
- Including this information in the supplemental material is fine, but if the main contribution of the paper involves human subjects, then as much detail as possible should be included in the main paper.
- According to the NeurIPS Code of Ethics, workers involved in data collection, curation, or other labor should be paid at least the minimum wage in the country of the data collector.

15. **Institutional review board (IRB) approvals or equivalent for research with human subjects**

Question: Does the paper describe potential risks incurred by study participants, whether such risks were disclosed to the subjects, and whether Institutional Review Board (IRB) approvals (or an equivalent approval/review based on the requirements of your country or institution) were obtained?

Answer: [NA]

Justification: [NA]

Guidelines:

- The answer NA means that the paper does not involve crowdsourcing nor research with human subjects.
- Depending on the country in which research is conducted, IRB approval (or equivalent) may be required for any human subjects research. If you obtained IRB approval, you should clearly state this in the paper.
- We recognize that the procedures for this may vary significantly between institutions and locations, and we expect authors to adhere to the NeurIPS Code of Ethics and the guidelines for their institution.
- For initial submissions, do not include any information that would break anonymity (if applicable), such as the institution conducting the review.

16. **Declaration of LLM usage**

Question: Does the paper describe the usage of LLMs if it is an important, original, or non-standard component of the core methods in this research? Note that if the LLM is used only for writing, editing, or formatting purposes and does not impact the core methodology, scientific rigor, or originality of the research, declaration is not required.

Answer: [NA]

Justification: [NA]

Guidelines:

- The answer NA means that the core method development in this research does not involve LLMs as any important, original, or non-standard components.
- Please refer to our LLM policy (<https://neurips.cc/Conferences/2025/LLM>) for what should or should not be described.

A Environment and dataset configurations

In this section, we describe the environments and datasets used in our experiments, covering three distinct domains: I-PHYRE, N-body simulations, and the PHYRE physical reasoning benchmark. Each environment presents unique challenges and dynamics, requiring tailored data generation and simulation procedures. We outline the structure of the training, within-scenario, and cross-scenario datasets, along with the physical parameters and recorded features essential for model training and evaluation. These configurations ensure both diversity and rigor in testing the generalization capabilities of our models across varying physical setups.

A.1 I-PHYRE

We adopt the original settings from the I-PHYRE work (Li et al., 2023). The training dataset consists of 10 basic games: support, hinder, direction, hole, fill, seesaw, angle, impulse, pendulum, and spring. For each game, we randomly generate 5 successful and 5 failed action sequences. The within-scenario setting includes an additional 10 successful and 10 failed action sequences for each of the 10 basic games. The cross-scenario setting contains 10 successful and 10 failed action sequences from 30 unseen games, which include 10 noisy games, 10 compositional games, and 10 multi-ball games. All object masses are set to be equal, and small friction and elasticity coefficients are applied. For each game, we record the center positions, lengths, angles, radii, horizontal velocities, vertical velocities, and rotational velocities of each object, as well as the spring pair indices. Each sequence contains up to 12 objects and spans 150 timesteps.

A.2 N-body

We employed the REBOUND engine to simulate N-body dynamics and considered two types of N-body problems for 3D trajectories: the planetary n-body problem and the cometary n-body problem. In the planetary n-body problem, the comets are initialized with Keplerian velocities, while in the cometary n-body problem, the planets are initialized with escape velocities. Initial positions are sampled from the spherical coordinate system and then converted to Cartesian coordinates. For the training and within-scenario datasets, the radii are sampled within the range of 1 to 3, azimuthal angles are sampled from 0 to 2π , and polar angles are sampled from $-\pi/6$ to $\pi/6$. Masses for the orbiting bodies are sampled from 0.05 to 0.1, while the central massive body is assigned a mass sampled from 3 to 5 or from 7 to 9. All sampling is performed using Latin Hypercube Sampling to ensure comprehensive space coverage, even with sparse samples. The training dataset includes 50 two-body planetary trajectories (1 orbiting body), 50 three-body planetary trajectories (2 orbiting bodies), 50 two-body cometary trajectories (1 orbiting body), and 50 three-body cometary trajectories (2 orbiting bodies), spanning across 50 timesteps. The within-scenario dataset consists of the same four trajectory types as the training set but with different initial conditions, with trajectories spanning 150 timesteps. The cross-scenario dataset contains 50 eight-body planetary trajectories, 50 ten-body planetary trajectories, 50 eight-body cometary trajectories, and 50 ten-body cometary trajectories. For these cross-scenario trajectories, initial radii are sampled from 1 to 5, masses of the orbiting bodies are sampled from 0.05 to 0.15, and the central body mass is sampled from 3 to 9. The trajectory length in the cross-scenario data is 150 steps. We record the masses, 3D Cartesian coordinates, and velocities for training.

A.3 PHYRE

We conduct experiments on the PHYRE-B tier, using the standard split from fold 1—one of the most challenging folds indicated by its low baseline performance. The goal is to make the green ball touch the purple or blue objects by placing a red ball. This physical reasoning benchmark presents a high level of difficulty for several key reasons. First, it features a diverse range of objects—such as balls, bars, sticks, and jars—with varying shapes and uneven mass distributions, adding complexity to interaction dynamics. Second, the solution space is extremely narrow relative to the vast array of possible actions, rendering random attempts largely ineffective. Third, achieving the goal requires navigating a sequence of intricate physical events, including toppling, rotation, collisions, and frictional forces. We train the model using 20 within-template scenarios, each containing 20 tasks, with 30 actions allocated per task. The model is evaluated on the remaining 5 templates, which were not seen during training. For each sample, we simulate dynamic frames at 256×256 resolution using a

stride of 60 and extract object masks for supervision. To ensure stable training, we also record initial linear and angular velocities for each training chunk. To visualize the force field, we place red balls on a 64×64 grid, run simulations to generate trajectories, and compute second derivatives as field vectors using finite difference methods.

B Training details

B.1 Hyperparameters

In I-PHYRE, we train the models using a single NVIDIA A100 Tensor Core 80GB GPU. The force field predictor in NFF is based on a DeepONet architecture, consisting of trunk and branch networks, each a 3-layer MLP with a hidden size of 256. The ODE solver uses the Euler method with a step size of 0.005. The 150-step trajectories are divided into 6-step segments, with 6 trajectories per batch. The learning rate starts at $5e-4$ and gradually decays to $1e-5$ following a cosine annealing schedule. Training occurs over 3000 epochs with a weight decay of $1e-5$ for regularization.

The interaction predictor in IN is a 3-layer MLP with a hidden size of 256, while the decoder is also an MLP of the same size. SlotFormer uses 3 transformer encoder layers, each with 4 attention heads and a feedforward network of size 256. Both IN and SlotFormer are trained with a batch size of 50 trajectories, employing the same segmentation technique. All other hyperparameters are kept consistent with those used in NFF.

In N-body, we train the models using a single NVIDIA GeForce RTX 3090 GPU. For all models, the 50-step trajectories are divided into 5-step segments, with 50 trajectories per batch. The learning rate starts at $5e-4$ and gradually decays to $1e-7$ following a cosine annealing schedule. Training occurs over 5000 epochs with a weight decay of $1e-5$ for regularization. All the other hyperparameters are the same as those used in I-PHYRE.

For training the vision-based NFF in PHYRE, we perform feature extraction from 256×256 object masks using four sparse convolutional layers with channel sizes of 16, 32, 32, and 32. The model architecture includes a DeepONet, composed of a trunk network and a branch network, each with 3 layers and 128 hidden units. DeepONet takes as input a combination of mask, positional, and velocity features, and outputs the corresponding 2D forces and torques acting on each object. Then, we perform a transform and rotation on the object masks to obtain the frames in the next states. The ODE solver uses the Euler method with a step size of 0.025. We adopt a cosine annealing schedule to adjust the learning rate from $3e-4$ to $5e-5$, with a batch size of 8. Training is conducted for 500 epochs to ensure convergence, with the 18-step trajectories divided into 2-step segments during training.

B.2 Evaluation metrics

In this study, the chosen evaluation metrics include, RMSE, FPE, PCE, and R. Each of these metrics provides valuable insights into different characteristics of the model’s predictions, allowing for a comprehensive evaluation.

Root Mean Squared Error (RMSE) The RMSE, the square root of MSE, shares the same characteristics as MSE in terms of penalizing larger errors. However, it provides the error in the same units as the original data, allowing for a more intuitive understanding of how far off the model’s predictions are, on average, in the context of physical trajectories:

$$\text{RMSE} = \sqrt{\frac{1}{n} \sum_{t=1}^n (\hat{z}_t - z_t)^2}. \tag{A1}$$

Final Position Error (FPE) The FPE specifically measures the discrepancy between the predicted and actual final position of the object at the end of the trajectory. This metric is crucial for goal-driven physical reasoning tasks where the objects are expected to finally move into a specific area. FPE helps ensure that the model is not only capturing the intermediate trajectory but also predicting the final destination with high accuracy:

$$\text{FPE} = |\hat{z}_{\text{final}} - z_{\text{final}}|. \tag{A2}$$

Table A1: **Results of different kinds of integration methods.** The computational complexity of the model is proportional to the number of average integration steps (relative to Euler $5e-3$). Among non-adaptive methods, with the increase of computational complexity, the Heun3 method achieves the best performance. For uniformity across tasks and stability during training, we simply selected the Euler method for integration.

Method	Average steps (relative)	Within	Cross
Adaptive methods (tolerance)			
Adaptive ($1e-4$)	0.28	0.091 ± 0.008	1.100 ± 0.021
Adaptive ($1e-5$)	0.36	0.093 ± 0.008	1.063 ± 0.020
Adaptive ($1e-6$)	0.56	0.107 ± 0.008	1.082 ± 0.023
Adaptive ($1e-7$)	1.07	0.119 ± 0.009	1.125 ± 0.026
Non-adaptive methods (step size)			
Euler ($5e-3$)	1.00	0.139 ± 0.013	1.090 ± 0.023
Midpoint ($5e-3$)	2.00	0.091 ± 0.009	1.040 ± 0.023
Heun3 ($5e-3$)	3.00	0.091 ± 0.008	1.022 ± 0.022
RK4 ($5e-3$)	4.00	0.103 ± 0.009	1.084 ± 0.029

Position Change Error (PCE) The PCE quantifies the error in the predicted change of position over time, which can be interpreted as a measure of the model’s accuracy in tracking the object’s velocity during its motion:

$$\text{PCE} = |\Delta \hat{z}_t - \Delta z_t|. \tag{A3}$$

Pearson Correlation Coefficient (R) The R measures the linear relationship between the predicted and actual trajectories. R is useful for assessing how well the model captures the overall trend or pattern of the trajectory, even when the absolute errors might vary. A high correlation suggests that the model is effectively tracking the overall movement, while a low correlation might indicate that the model fails to capture the underlying trajectory pattern:

$$R = \frac{\sum_{t=1}^n (\hat{z}_t - \bar{\hat{z}})(z_t - \bar{z})}{\sqrt{\sum_{t=1}^n (\hat{z}_t - \bar{\hat{z}})^2 \sum_{t=1}^n (z_t - \bar{z})^2}}. \tag{A4}$$

C Ablation studies on integration methods

In [Tab. A1](#), we present additional ablation studies comparing various integration methods. Specifically, we evaluate the performance of different integration orders on the N-body task, including Euler, Midpoint, Heun3, RK4, and adaptive methods. Computational complexity is measured by the average number of integration steps. The results indicate that Heun3 excels in within-scenario and cross-scenario generalization. Despite this, Euler integration has lower computational complexity than the higher-order methods, while maintaining better training stability compared to adaptive methods. These findings suggest that Euler integration is sufficient for our physical reasoning tasks.

D Comparison of baselines under noise

We evaluate the robustness of our model under noisy conditions by introducing noise at varying levels to the N-body simulated trajectories during training. As shown in [Tab. A2](#), NFF demonstrates consistently strong performance across both within-scenario and cross-scenario settings. In contrast, IN tends to diverge significantly from the ground truth, particularly in the cross-scenario case, where it exhibits large errors.

Additionally, to simulate imperfect perception in I-PHYRE, we extract object states from raw RGB images using OpenCV. The results in [Tab. A3](#) indicate that NFF continues to perform better than other models in zero-shot planning scenarios.

E Planning time on N-body

We demonstrate how backward integration accelerates planning in N-body tasks. As shown in [Tab. A4](#), backward planning is up to 10 times faster than traditional optimization-based planning methods.

Table A2: **NFF demonstrates stronger robustness than other models under imperfect perception.** For N-body, we introduced random noise of 1% to 3% to the training data to mimic imperfect simulation.

Model	Within			Cross		
	w/o noise	1% noise	3% noise	w/o noise	1% noise	3% noise
IN	0.31 ± 0.02	0.33 ± 0.03	0.50 ± 0.03	4.73 ± 0.11	2.71 ± 0.06	8.63 ± 0.78
SlotFormer	0.26 ± 0.02	0.26 ± 0.02	0.37 ± 0.03	3.53 ± 0.13	3.49 ± 0.15	2.29 ± 0.04
NFF	0.14 ± 0.01	0.12 ± 0.01	0.13 ± 0.01	1.09 ± 0.02	1.32 ± 0.04	1.53 ± 0.03

Table A3: **Probability of success in I-PHYRE under noisy perception.** We use OpenCV to extract states from raw RGB images and then evaluate the model’s zero-shot success rate on cross-scenario games.

Model	Ground-truth states	RGB images
Random	0.24 ± 0.04	0.24 ± 0.04
IN	0.25 ± 0.06	0.25 ± 0.06
SlotFormer	0.30 ± 0.07	0.23 ± 0.06
NFF	0.51 ± 0.08	0.41 ± 0.08

Table A4: **NFF enables fast planning through backward integration.** NFF performs planning approximately 10 times faster than optimization-based methods in the N-body task. The value represents the time in seconds required to plan 200 scenarios in parallel, with each experiment conducted three times.

Model	Type	Within	Cross
IN	Optimization	13.886 ± 0.225	11.693 ± 0.153
SlotFormer	Optimization	22.098 ± 0.156	22.489 ± 0.068
NFF	Backward integration	1.717 ± 0.023	1.716 ± 0.013

F Detailed planning results

We present the detailed planning results of different models across trials in [Tab. A5](#).

Besides those dynamic prediction models, we also benchmark the planning performance of the large language model GPT-4o with the refinement mechanism. The core idea is utilizing In-Context Learning (ICL) abilities and high-level reasoning abilities of large language models to find correct solutions.

The prompt in Round 1 consists of 3 parts: (1) I-PHYRE description and an elaborately explained example. (2) Other training examples. (3) Description of the testing game setting. In Part 2, we provide GPT-4o with 1 successful solution and 1 wrong solution together with resulting trajectories of objects for each of the 10 basic games. In the refinement stage (*i.e.*, Round 2 and Round 3), we run the action sequence proposed by GPT-4o on the simulator, Then we offer GPT-4o the resulting trajectory and ask it to modify the previous solution or design a new one.

We test the performance of GPT-4o for both within-scenario planning and cross-scenario planning. Detailed results are presented in [Tab. A6](#). Within-scenario games contains the same 10 games used in the prompt in Round 1. So the language model can memorize corresponding solutions provided in the prompt to achieve good performance. Cross-scenario games contains the other 30 game settings, on which the performance of GPT-4o is better than other baselines (Random, IN, SlotFormer) in [Tab. A5](#). The improvement of performance through refinement is witnessed in both within-scenario and cross-scenario games.

The prompt used in Round 1 is shown below.

Table A5: **Planning results in I-PHYRE**. Average probability of succeeding cross-scenario games after n trails from IN, SlotFormer, NFF, human, w/o refining. The gray line indicates the best results among all the AI methods.

Method	Refine	Round 1	Round 2	Round 3	Round 4	Round 5
Random	-	0.24 ± 0.04	0.37 ± 0.05	0.45 ± 0.06	0.51 ± 0.06	0.56 ± 0.06
IN	×	0.25 ± 0.06	0.33 ± 0.07	0.39 ± 0.07	0.42 ± 0.08	0.45 ± 0.08
IN	✓	0.25 ± 0.06	0.39 ± 0.07	0.48 ± 0.07	0.57 ± 0.07	0.63 ± 0.06
SlotFormer	×	0.30 ± 0.07	0.36 ± 0.08	0.39 ± 0.08	0.41 ± 0.08	0.43 ± 0.08
SlotFormer	✓	0.30 ± 0.07	0.42 ± 0.08	0.49 ± 0.07	0.55 ± 0.07	0.60 ± 0.07
NFF	×	0.51 ± 0.08	0.55 ± 0.08	0.58 ± 0.08	0.60 ± 0.08	0.62 ± 0.08
NFF	✓	0.51 ± 0.08	0.62 ± 0.08	0.69 ± 0.07	0.74 ± 0.06	0.77 ± 0.06
Human	×	0.52 ± 0.06	0.66 ± 0.06	0.73 ± 0.06	0.77 ± 0.06	0.80 ± 0.05
Human	✓	0.52 ± 0.06	0.70 ± 0.06	0.79 ± 0.05	0.83 ± 0.04	0.86 ± 0.04

Table A6: **GPT-4o's planning results in I-PHYRE**. The GPT-4o refines itself after each round of play and shows increasingly better performance.

Scenario	Round 1	Round 2	Round 3
Within	0.74 ± 0.08	0.78 ± 0.07	0.82 ± 0.07
Cross	0.35 ± 0.07	0.45 ± 0.08	0.51 ± 0.04

/* PART 1 */

This is a 2D physics simulation environment. There will be one or few red balls, and may appear black blocks, grey blocks and blue blocks. Lengths of blocks are different.

All these objects are rigid bodies. When we talk about physical laws, we consider gravity (there is gravity in this environment), friction (but the friction coefficients are small), collision between rigid bodies, rotation of balls and blocks.

However, grey blocks and black blocks are fixed and stay still to their initial positions. They do not apply any laws of physics (even collision won't affect them). The red ball and blue blocks are controlled by physical laws.

Initially, all objects are at rest (their velocity and angular velocity are all 0).

There may exist 2 types of constraints between two objects: spring or joint. "Spring" constraint means there is a spring linking 2 objects. Springs in all the games have the same rest length, stiffness and damping rate (You can infer these properties from trajectories provided below that contain springs). "Joint" constraint means there is a rod supporting 2 objects so their distance is fixed.

We emphasize that grey and black blocks are not affected by any constraints. They are fixed to their initial positions.

Now, we are going to play a game. The goal is to make all the red balls fall down to the bottom of the canvas.

Let's first define a coordinate on the canvas. Let the origin be the top left corner. The x-axis is horizontal, from left to right. The y-axis is vertical, from top to bottom. The canvas size is (600, 600), so the coordinate of the lower-right corner is (600, 600).

The only operation the player can do is to eliminate any grey blocks at any time they want (however, we limit the whole game in 15 seconds. If after 15s the red ball still doesn't reach the bottom, the player loses the game). The player cannot eliminate other objects, including the red ball, blue or black blocks. Note that if the player eliminates a grey block which is connected to some other object with a spring or joint, then the spring/joint between them will disappear.

Now, I will show you a game named "fill". The name is actually the key to solve this problem. In this game, a blue block is placed above a grey block. You need to eliminate the grey block so that the blue block falls down to fill the pit on the "ground" (the ground and pit are built by a few black blocks). Otherwise, the red ball will roll into and get trapped in the pit.

Below is the initial setting of the game. I will describe the meaning of each parameter.

```
{'block': [[[100.0, 420.0], [400.0, 420.0]], [[100.0, 400.0], [250.0, 400.0]], [[350.0, 400.0], [400.0, 400.0]], [[270.0, 200.0], [330.0, 200.0]], [[270.0, 180.0], [330.0, 180.0]], [[100.0, 150.0], [180.0, 200.0]], [[150.0, 100.0], [150.0, 150.0]]], 'ball': [[120.0, 120.0, 20.0]], 'eli': [0, 0, 0, 1, 0, 1, 1, 0], 'dynamic': [0, 0, 0, 0, 1, 0, 0, 1]}
```

First comes the 'block' items. Each item is in the form of '['left_x, left_y], [right_x, right_y]', namely, the coordinates of the left and right corner of the block. Note that each block is generated by moving a circle (radius = 10) centered from the left corner to the right corner.

Next comes the 'ball' items. Now we only have 1 ball in this game. This item looks like '[x, y, r]', namely, the coordinates of the center and the radius of the ball.

Then comes the 'eli' item specifying which of these objects are eliminable. In this game, 'eli': [0, 0, 0, 1, 0, 1, 1, 0]. This is an 8-dimensional vector. The first 7 elements describes the 7 blocks (there are 7 elements in the 'block' item), and the last element describes the ball. 0 means the object is not eliminable, and 1 means the object is eliminable.

Finally comes the 'dynamic' item, which specifies whether the objects are dynamic. In this game, 'dynamic': [0, 0, 0, 0, 1, 0, 0, 1]. The first 7 elements are the 7 blocks, and the last element is the ball. 0 means the object is static (not apply physical laws), and 1 means the object is dynamic (apply physical laws).

You can infer from 'eli' and 'dynamic' that the 4th, 6th, and 7th blocks are grey, the 5th block is blue. All other blocks are black.

In other game settings, there may exist 'spring' or 'joint' items. They look like 'spring': [[6, 7]], which means there is only 1 spring connecting the 6th and 7th object (object can be blocks or balls). 'joint': [[6, 7]] means there is only 1 joint connecting the 6th and 7th object.

Here, we also provide an image of the game.

<image here>

Now you are provided with a successful action sequence that can solve the game. The action sequence is as follows:

```
[[150.0, 125.0, 0.3], [300.0, 200.0, 1.4000000000000004]]
```

Action sequence is a list of eliminations [pos_x, pos_y, t], where 'pos_x' and 'pos_y' must be the center of some block (formally, the center is the average of the coordinates of 2 corners: $pos_x = 1 / 2 * (left_x + right_x)$, $pos_y = 1 / 2 * (left_y + right_y)$), and 't' is the time when the block is eliminated (t should be in 0.1 ~ 15.0). In this example, there are 2 grey blocks to eliminate. [150, 125, 0.3] means eliminate the vertical block (next to the red ball) at t = 0.3s; [300.0, 200.0, 1.4] means eliminate the horizontal block (which supports the blue block from falling down) at t = 1.4s.

In this setting, all positions that can be eliminated are [[300.0, 200.0], [140.0, 175.0], [150.0, 125.0]].

Now you are provided with the trajectory of the red ball and the dynamic (blue) block. Other blocks are either static (the same as in

the initial setting) or eliminated at some time. In this case, there is only one blue block. If there are multiple blue blocks, their position at some timestamp will be given by the same order as in 'dyn' item. If there are no blue balls, the 'dynamic' item will be an empty list.

Below is the trajectory.

```
t = 0.000s: {'ball': [[120.0, 120.0]], 'dynamic_block': [[270.0, 180.0, 330.0, 180.0]]}
t = 0.167s: {'ball': [[120.0, 121.25]], 'dynamic_block': [[270.0, 180.03, 330.0, 180.03]]}
t = 0.333s: {'ball': [[120.0, 125.28]], 'dynamic_block': [[270.0, 180.03, 330.0, 180.03]]}
...
```

/* PART 2 */

Now we provide you with more examples from different game settings. We will provide 10 game settings. For each game setting, we will provide you with the initial setting (data + image), and 2 action sequence & trajectory (including 1 successful and 1 failed ones).

Game 1: name:angle

```
Initial setting: {'block': [[100.0, 400.0], [400.0, 400.0]],
[[200.0, 350.0], [210.0, 350.0]], [[200.0, 300.0], [210.0, 300.0]],
[[480.0, 400.0], [550.0, 400.0]], [[390.0, 350.0], [400.0, 350.0]],
[[390.0, 300.0], [400.0, 300.0]], [[100.0, 380.0], [100.0, 360.0]],
[[550.0, 380.0], [550.0, 360.0]], [[200.0, 280.0], [400.0, 280.0]]],
'ball': [[300.0, 250.0, 20.0]], 'eli': [0, 1, 1, 0, 1, 1, 0, 0, 0, 0],
'dynamic': [0, 0, 0, 0, 0, 0, 0, 0, 0, 1, 1]}
Eliminable positions: [[205.0, 350.0], [205.0, 300.0],
[395.0, 350.0], [395.0, 300.0]]
Game setting image:
```

<image here>

Successful Case 1:

```
Action sequence: [[395.0, 300.0, 1.4000000000000004],
[205.0, 350.0, 2.9000000000000001], [205.0, 300.0,
3.90000000000000012], [395.0, 350.0, 5.9000000000000002]]
This action sequence leads to success.
Trajectory:
```

```
t = 0.000s: {'ball': [[300.0, 250.0]], 'dynamic_block':
[[200.0, 280.0, 400.0, 280.0]]}
t = 0.167s: {'ball': [[300.0, 250.32]], 'dynamic_block':
[[200.02, 280.3, 400.02, 280.3]]}
...
```

Failed Case 1:

```
Actions: [[395.0, 350.0, 3.0000000000000001], [205.0,
300.0, 4.8000000000000002], [205.0, 350.0, 6.4000000000000002], [395.0,
300.0, 6.7000000000000002]]
This action sequence leads to failure.
Trajectory:
```

```
t = 0.000s: {'ball': [[300.0, 250.0]], 'dynamic_block':
[[200.0, 280.0, 400.0, 280.0]]}
t = 0.167s: {'ball': [[300.0, 250.32]], 'dynamic_block':
[[200.02, 280.3, 400.02, 280.3]]}
...
```

... <more examples>

/* PART 3 */

Your goal is to provide a successful action sequence (that makes the red ball fall to the bottom of the canvas) under a new game setting. Below is the new game setting.

Game name: "angle".

Game setting:

...

Eliminable positions: ...

Game setting image:

<image here>

Your task is to provide a successful action sequence in the same format as examples given previously. You should make some analysis or explanations.

Now please provide one successful action sequence. At the end of your response, please give the entire action sequence in the format of

"

 Action sequence: [[pos_1_x, pos_1_y, t_1], [pos_2_x, pos_2_y, t_2], ...]

"

so that we can extract and test your proposed action sequence easily.

The prompt used in GPT-4o.

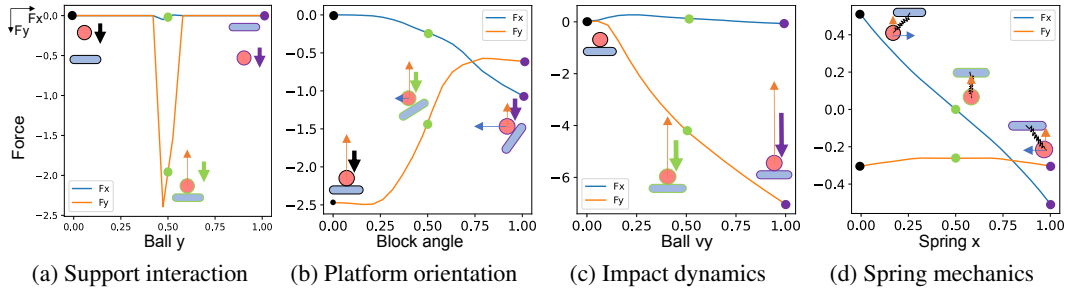


Figure A1: **Force response analysis under controlled state variations.** Each plot shows the predicted force components (F_x in blue, F_y in orange) from our trained NFF model, measured in normalized units against different state parameters. The subplots systematically analyze: (a) support forces as a function of ball height, showing characteristic contact response when the ball meets the platform, (b) force decomposition as the platform rotates from horizontal (0°) to vertical (90°), (c) impact forces scaling with the ball's downward velocity, and (d) spring forces varying with horizontal displacement from the equilibrium position. Each plot varies one parameter while keeping all other scene variables constant, demonstrating NFF's learned physical principles, including contact mechanics, geometric reasoning, impact dynamics, and harmonic motion.

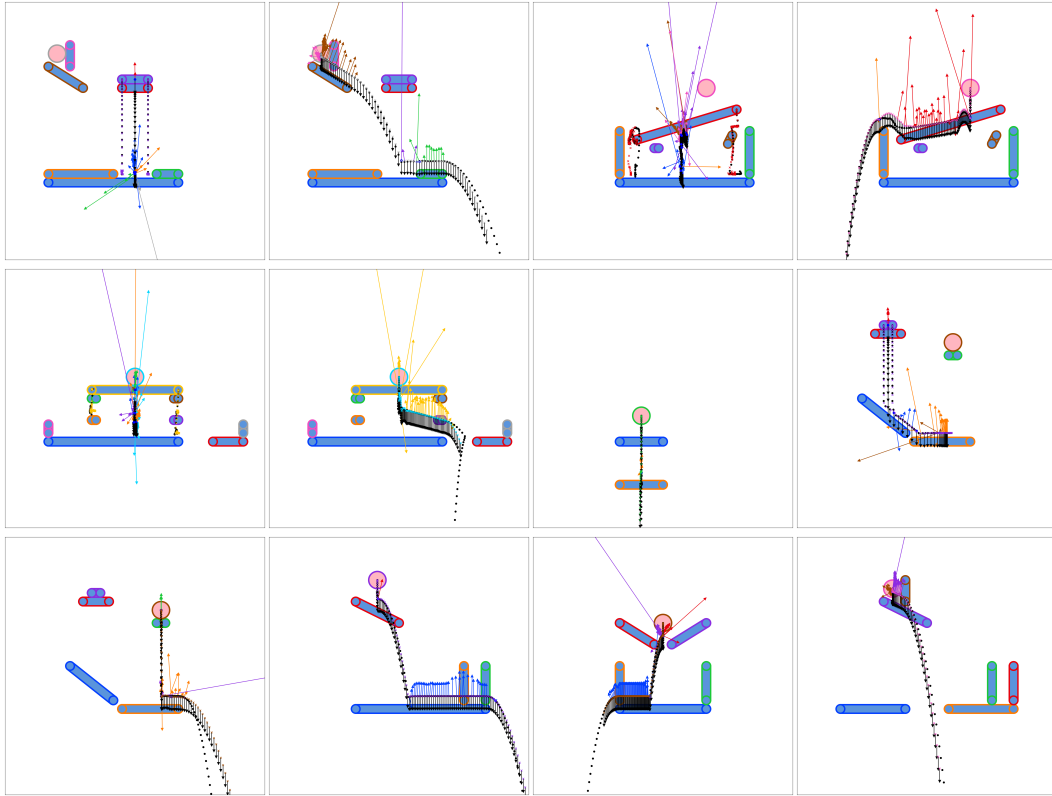


Figure A2: **The inverted forces from NFF and its predicted trajectories of dynamic objects in I-PHYRE within scenarios.** Ground-truth trajectories are represented by black dots, while predicted trajectories are shown with colorful dots. Horizontal and vertical forces are depicted as arrows, while rotational forces are indicated by red or blue dots, signifying negative and positive forces, respectively. The color of the forces indicates which object is exerting the force. Only the initial states are shown for static objects. Some objects will be eliminated during the process. Best seen in videos.

G More visualization

We provide additional visualizations of the learned forces along trajectories in I-PHYRE, as shown in Fig. A1, Fig. A2, and Fig. A3. Further prediction results on the N-body dataset are presented in Fig. A4. Additionally, examples of failure cases in NFF predictions are shown in Fig. A5. We also visualize the failure encoding of slot-attention in SlotFormer in Fig. A6.

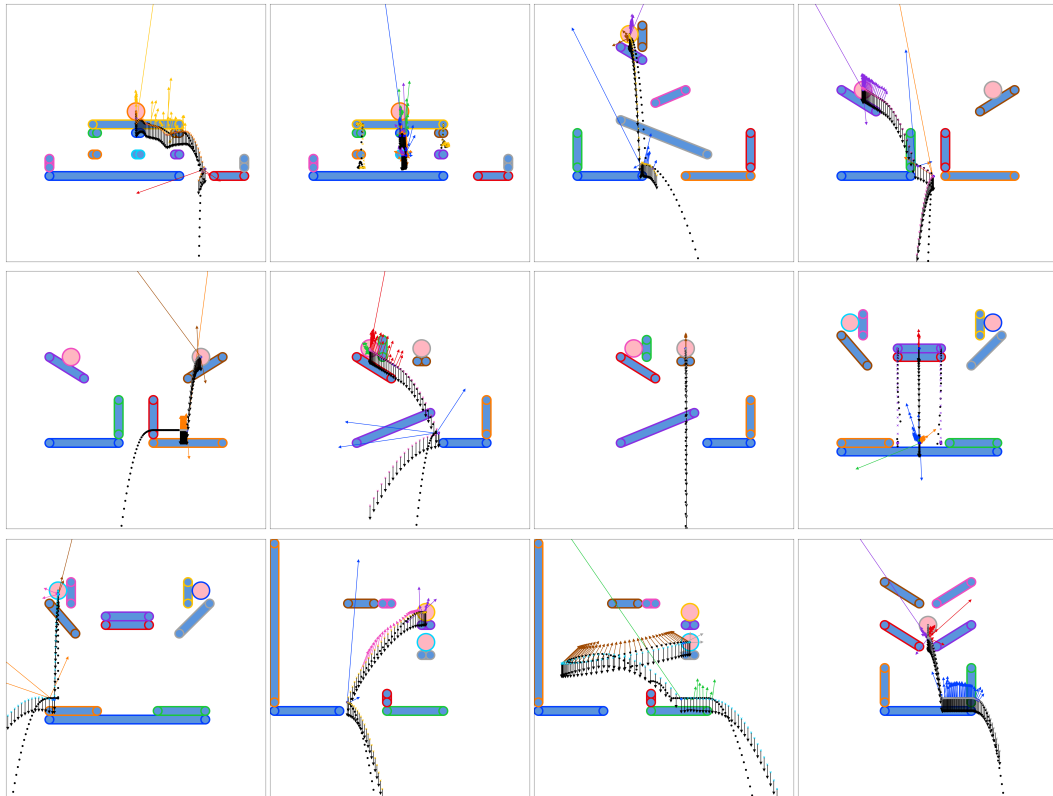


Figure A3: **The inverted forces from NFF and its predicted trajectories of dynamic objects in I-PHYRE cross scenarios.** Ground-truth trajectories are represented by black dots, while predicted trajectories are shown with colorful dots. Horizontal and vertical forces are depicted as arrows, while rotational forces are indicated by red or blue dots, signifying negative and positive forces, respectively. The color of the forces indicates which object is exerting the force. Only the initial states are shown for static objects. Some objects will be eliminated during the process. Best seen in videos.

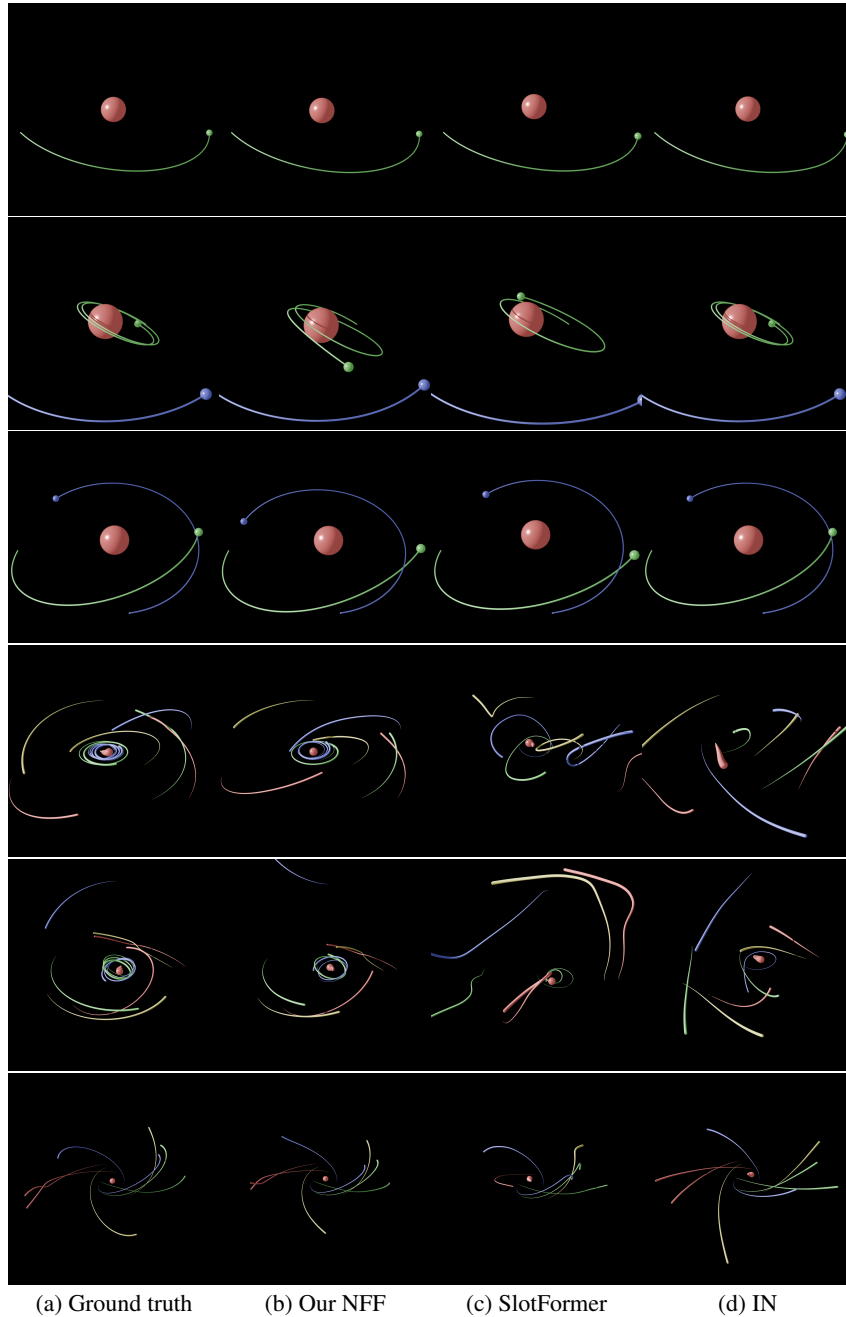


Figure A4: **Additional prediction results on N-body.** The figure displays predictions from simple N-body dynamics to complex dynamics with more bodies and extended prediction horizons.

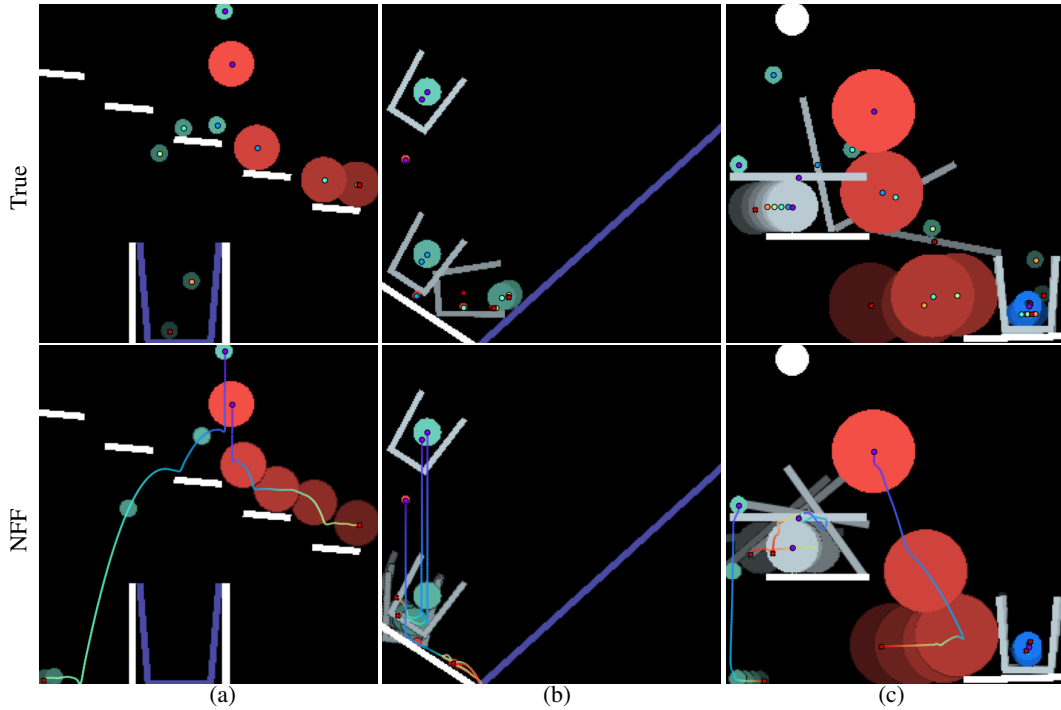


Figure A5: **Examples of prediction failures in PHYRE cross-scenario setting.** (a) Minor prediction inaccuracies accumulate, causing the green ball to fall out of the cup unexpectedly. (b) Extremely tiny red balls introduce unforeseen interactions, potentially resulting in significant dynamic changes, such as cup rotation. (c) Complex interactions between the ball and the seesaw can hinder accurate force prediction.

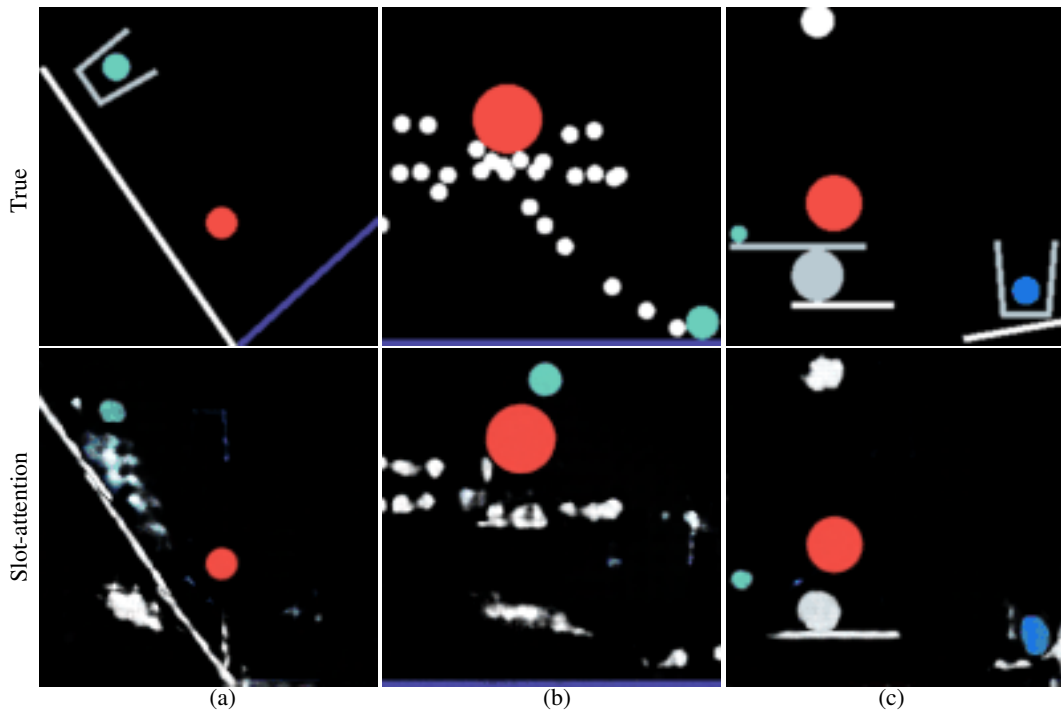


Figure A6: **Examples of failures in Slotformer's pretrained slot-attention module in cross-scenario setting.** The pretrained slot-attention encoder in slotformer, responsible for encoding visual features, exhibits poor generalization to cross-scenario scenes, leading to an inability to capture the precise geometric information crucial for physical reasoning.